Synthesis and Self-Assembly of Functionalized Hexa-*peri*-hexabenzocoronenes

Shunji Ito,[a] Mike Wehmeier,[a] J. Diedrich Brand,[a] Christian Kübel,[a] Rebekka Epsch,[b] Jürgen P. Rabe,*[b] and Klaus Müllen*[a]

Abstract: Monolayers of hexa-alkyl substituted derivatives of hexa-*peri*-hexabenzocoronene (HBC) **1b** have previously been investigated by scanning tunneling microscopy (STM) and scanning tunneling spectroscopy (STS). It is expected that different functional groups (electron donating or withdrawing) connected to the aromatic core will influence the packing pattern and possibly the current-voltage characteristics as well. In order to provide suitable model systems, a new synthetic approach to synthesize functionalized HBC derivatives has been developed. This was accomplished by [4+2]-cycloaddition of suitably bromo-substituted diphenylacetylenes and 2,3,4,5-tetraarylcyclopenta-2,4-dien-1-ones followed by an oxidative cyclodehydrogenation with iron(III) chloride/nitromethane. Using this strategy three different substitution patterns were synthesized: 2-bromo-5,8,11,14,17-pentadodecylhexa-*peri*-hexabenzocoronene (**2a**), 2,5-dibromo-8,11,14,17-pentadodecylhexa-*peri*-hexabenzocoronene (**2b**), and 2,11-dibromo-5,8,14,17-pentadodecylhexa-*peri*-hexabenzocoronene (**2c**). These bromo-substituted HBC derivatives were subjected to palladium catalyzed coupling reactions to give donor (alkoxy, amino) as well as acceptor (ester, cyano) substituted derivatives. The self-assembly of these new HBC derivatives was studied in the bulk as well as at an interface. DSC, optical microscopy, and X-ray diffraction revealed the existence of columnar mesophases. The bulk structure in the mesophase is largely insensitive to changes of the substitution pattern; however, in situ scanning tunneling microscopy at the solid-fluid interface between an organic solution of the HBC derivative and highly oriented pyrolytic graphite reveals different packing patterns of the first adsorbed monolayer.

Keywords: aromatic hydrocarbons · liquid crystals · mesophases · scanning tunnelling spectroscopy · self-assembly

Introduction

Polycyclic aromatic hydrocarbons (PAHs) with peripheral substituents such as alkoxy-substituted triphenylenes[1], rufigallols[2], or dibenzopyrenes[3] have been intensely studied in recent years. They consist of flat disc-type cores surrounded by flexible chains, which enable them to self-assemble into columnar mesophases.[4] The packing behavior of these discotic liquid crystals renders them well suited materials for the study of one-dimensional transport processes such as electrical conductivity[5] and photoconductivity[6] along the columnar axis. Using time-of-flight photoconductivity techniques as well as a pulse-radiolysis time-resolved microwave conductivity technique, it has been shown that highly ordered columnar phases of substituted triphenylenes exhibit a high charge carrier mobility.[7] By further increasing the size of the aromatic core, it should be possible to obtain an even higher charge carrier mobility. Indeed, we have recently shown, that soluble alkyl-substituted derivatives of hexa-*peri*-hexabenzocoronene (HBC)[8] (**1a–c**) exhibit a charge carrier mobility as high as 0.13 $cm^2 V s^{-1}$ in the mesophase[9]—the largest values determined so far for a discotic liquid crystalline material (Figure 1).

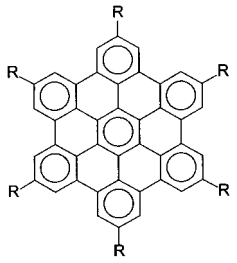

Figure 1. Hexaalkyl-substituted hexa-*peri*-hexabenzocoronenes **1a–c**.

Research toward electronics on the scale of individual molecules can be performed by investigating highly ordered monomolecular adsorbate layers of PAHs. Using the scanning tunneling microscope, single

[a] Prof. Dr. K. Müllen, Dr. S. Ito, Dr. M. Wehmeier, Dr. J. D. Brand, Dr. C. Kübel
Max-Planck-Institute for Polymer Research
Ackermannweg 10, 55128 Mainz (Germany)
Fax: (+49) 6131-379100
E-mail: müllen@mpip-mainz.mpg.de

[b] Prof. Dr. J. P. Rabe, Dr. R. Epsch
Humboldt University Berlin, Department of Physics
Invalidenstrasse 110, 10115 Berlin (Germany)
Fax: (+49) 30-20937632
E-mail: rabe@physik.hu-berlin.de

  0947-6539/00/0623-4327 $ 17.50+.50/0

molecules in these two-dimensional patterns can be visualized with submolecular resolution.[10–14] At the same time, information on their electronic properties can be obtained. For instance, it was possible to measure different current-voltage curves for the aromatic and aliphatic moieties of hexaalkyl-substituted hexa-*peri*-hexabenzocoronenes.[13]

It is tempting to subject HBCs to functionalization and investigate the influence of the molecular structure upon supramolecular ordering in both two-dimensional- and three-dimensional motives. In order to provide suitable systems, we have therefore synthesized HBC derivatives with electron donating and electron withdrawing substituents. HBCs with electron donating substituents provide a further prospect for better photoconductive properties in the discotic mesophase.[7]

Our recently published synthetic concept to obtain alkyl-substituted HBCs[8] consisted of an oxidative cyclodehydrogenation of substituted hexaphenylbenzenes with aluminum chloride/copper(II) trifluoromethanesulphonate (Cu-triflate) in carbon disulfide. However, applying these conditions and various other oxidizing agents[15] to hexaphenylbenzenes with substituents other than alkyl groups, we were not able to obtain the desired PAHs. With iron(III) chloride/nitromethane in dichloromethane we now introduce a cyclodehydrogenation system that allowed us to synthesize bromo-substituted hexa-*peri*-hexabenzocoronenes **2a–c** (Figure 2).

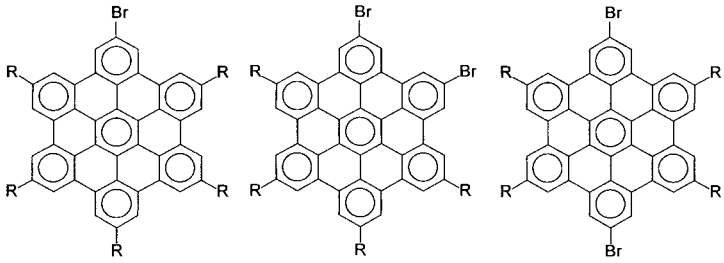

Figure 2. Bromo-substituted hexa-*peri*-hexabenzocoronenes **2a–c**.

Having at hand compounds **2a–c**, it is possible to exchange the bromo substituents at the aromatic core to introduce various electron donating and electron withdrawing groups. The liquid crystalline behavior of the new compounds is presented, and their self-assembly in ordered molecular patterns in monolayers at solid–fluid interfaces is investigated by scanning tunneling techniques.

Results

Synthesis

From a symmetry point of view, we recently considered the hexagonal structure of **1** as "superbenzene"[16] and analogous larger structures as "supernaphthalene" and "supertriphenylene". Here, we will try to create a benzene-like chemistry for the "superbenzene"-molecule. Since the parent hexa-*peri*-hexabenzocoronene (HBC) is insoluble in most common solvents, flexible, solubilizing substituents are a prerequisite for any chemical transformations at the aromatic core.

Originally, we synthesized hexaalkyl substituted hexa-*peri*-hexabenzocoronenes[8] starting from dialkyldiphenylacetylenes **3a** (Scheme 1). After a dicobalt octacarbonyl catalyzed cyclotrimerization, the resulting hexaalkyl hexaphenylbenzenes **4a** could be cyclodehydrogenated with aluminum chloride/copper triflate in carbon disulfide to give the desired PAHs **1**.

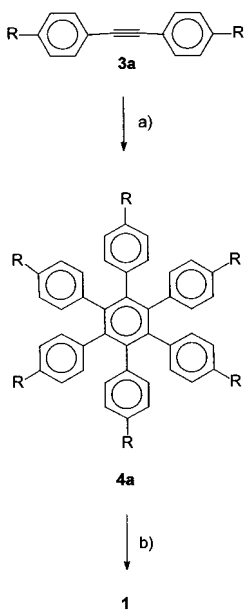

Scheme 1. Synthesis of hexaalkyl-substituted hexa-*peri*-hexabenzocoronenes **1**. a) $Co_2(CO)_8$, dioxane, reflux (92%); b) $AlCl_3$, $Cu(OSO_2CF_3)_2$, CS_2, RT (49%).

This synthetic concept allows only identical functionalization of all six phenyl substituents of the hexaphenylbenzene, or product mixtures have to be tolerated.[17] In order to get selectively functionalized products we turned to a different synthetic approach. This was accomplished by [4+2]-cycloaddition of suitably substituted diphenylacetylenes and 2,3,4,5-tetraarylcyclopenta-2,4-dien-1-ones to afford well defined hexaphenylbenzene derivatives[18] in excellent yields. With the right combination of diphenylacetylene and tetraarylcyclopentadienone, the intermolecular Diels–Alder reaction followed by a cyclodehydrogenation offers the possibility of synthesizing a variety of functionalized hexa-*peri*-hexabenzocoronenes for spectroscopic and electronic investigations. In a first attempt, we synthesized the pentaalkyl-substituted hexabenzocoronene **1d**, which we planned to modify at the free position at the HBC core by typical aromatic substitution reactions. However, neither nitration, bromination, nor Friedel–Crafts reactions gave the desired products. During nitration and Friedel–Crafts, reactions decomposition took place due to the strongly acidic conditions. Attempts to brominate **1d** resulted in inseparable mixtures of multiply brominated compounds. We then decided to build up several bromo-substituted hexabenzocoronenes by cyclodehydrogenation of the corresponding bromo-substituted hexaphenylbenzenes. The necessary bromo-hexaphenylbenzene derivatives were synthesized by Diels–Alder reactions of suitably substituted diphenylacetylene and tetraarylcyclopentadienone building blocks in a straightforward reaction sequences.

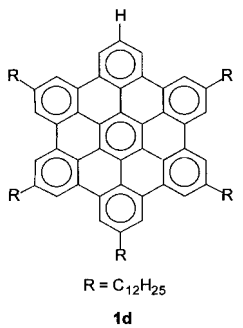

Figure 3. Pentaalkyl-substituted hexa-*peri*-hexabenzocoronene (**1d**).

4,4′-Dibromodiphenylacetylene (**3b**) was synthesized according to a literature procedure.[19] Attempts to prepare

0947-6539/00/0623-4328 $ 17.50+.50/0 *Chem. Eur. J.* **2000**, *6*, No. 23

the 4,4′-didodecyldiphenylacetylene (**3a**) from **3b** under Kumada[20] coupling conditions were unsuccessful, so we synthesized **3a** via a different reaction path (Scheme 2). This was achieved by introducing alkyl groups to 4,4′-dibromostilbene (**5a**)[21] in a quantitative Kumada coupling reaction with $NiCl_2$(dppp) as catalyst. After bromination of the stilbene double bond, the resulting precursor **6** could be transformed quantitatively into the desired dialkyldiphenylacetylene **3a** by treatment with potassium *tert*-butanolate in refluxing *tert*-butanol (Scheme 2).

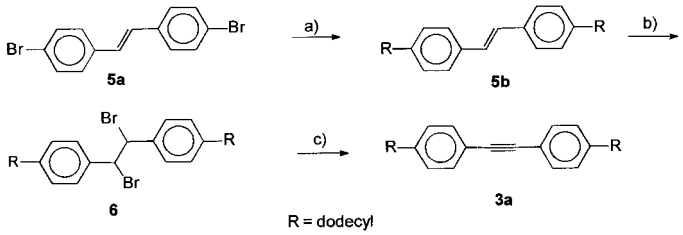

Scheme 2. Synthesis of dialkyl-substituted diphenylacetylene **3a**. a) $NiCl_2$(dppp), Et_2O (92%); Br_2, CCl_4, RT (90%); c) *tert*-butanol, potassium *tert*-butanolate, reflux (69%).

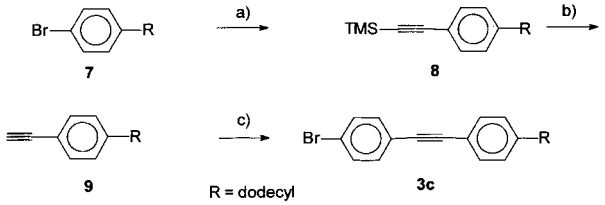

Scheme 3. Synthesis of unsymmetrically substituted diphenylacetylene **3c**. a) Pd^0, Et_3N, trimethylsilyacetylene, 65 °C (89%); b) THF, potassium fluoride, RT (95%); c) Pd^0, Et_3N, 4-bromo-iodobenzene, 65 °C (74%).

Synthesis of 4-bromo-4′-dodecyldiphenylacetylene (**3c**) was accomplished by a sequence of Sonogashira coupling reactions[22] (Scheme 3). First, 4-bromododecylbenzene (**7**)[23] was coupled with trimethylsilylacetylene to give **8** in 89% yield. After quantitative deprotection of the triple bond with potassium fluoride in DMF,[24] alkyne **9** was coupled with 4-bromo-iodobenzene yielding the unsymmetrically substituted building block **3c** (74%). Oxidation of the above synthesized 4,4′-dodecyldiphenylacetylene (**3a**) with I_2 in DMSO[25] at 155 °C resulted in the 1,2-diketone **11** and our improved synthesis of 1,3-diarylacetones **13a,b**[26] enabled the synthesis of the substituted tetraarylcyclopentadienones **14a,b** (Scheme 4).[27]

Two-fold Knoevenagel condensation of **11** and **13a,b** in refluxing ethanol yielded the tetraarylcyclopentadienone building blocks **14a,b** (48–67%). Suitable combinations of the synthesized diphenylacetylenes and tetraarylcyclopentadienones were then reacted in a [4+2]-cycloaddition in refluxing diphenylether to give hexaphenylbenzenes **4b–d** in good yields (70–75%).

Thus, **4b** and **4c** were available by reaction of tetra(4′-alkylaryl)cyclopentadienone **14a** with monobromo-**3c** and dibromodiphenylacetylene (**3b**), respectively (Scheme 5), whereas compound **4d** was synthesized with 3,4-bis(4′-alkyl-

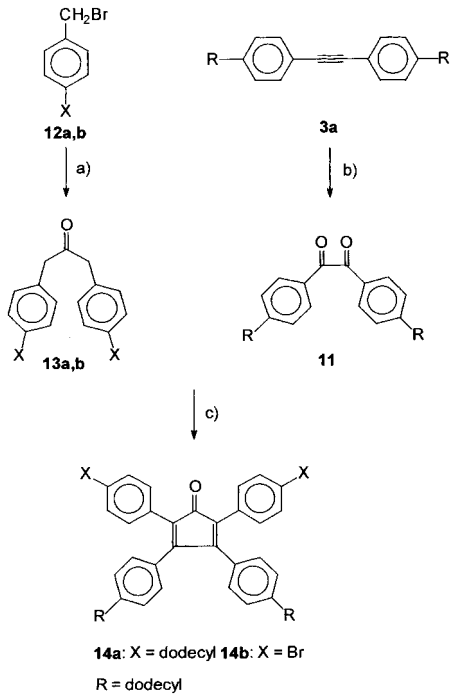

Scheme 4. Synthesis of substituted tetraarylcyclopentadienones **14a,b**. a) $Fe(CO)_5$, KOH, benzyltriethylammoniumchloride, CH_2Cl_2, H_2O, reflux (47–53%); b) I_2, DMSO, 155 °C (69%); c) KOH, EtOH, reflux, 5 min (43–60%).

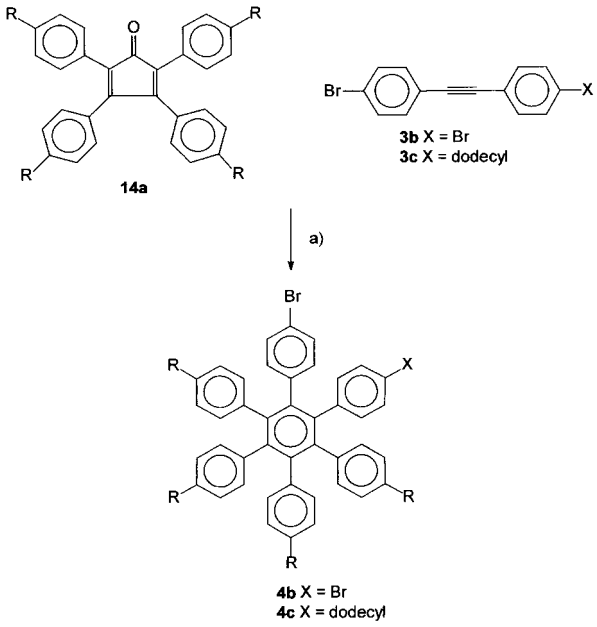

Scheme 5. Synthesis of bromo-substituted hexaphenylbenzenes **4b,c**. a) Diphenylether, reflux (71–76%).

aryl)-2,5-bis(4′-bromoaryl)cyclopentadienone(**14b**) and dialkyldiphenylacetylene **3a** (Scheme 6). All hexaphenylbenzenes could be unambiguously characterized by NMR spectroscopy, mass spectrometry and elemental analysis.

As mentioned in the introduction, we attempted to transform the functionalized hexaphenylbenzenes into the corresponding hexa-*peri*-hexabenzocoronene derivatives by applying the cyclodehydrogenation conditions ($AlCl_3$/Cu-triflate in CS_2) suitable for synthesizing hexaalkyl-substituted deriva-

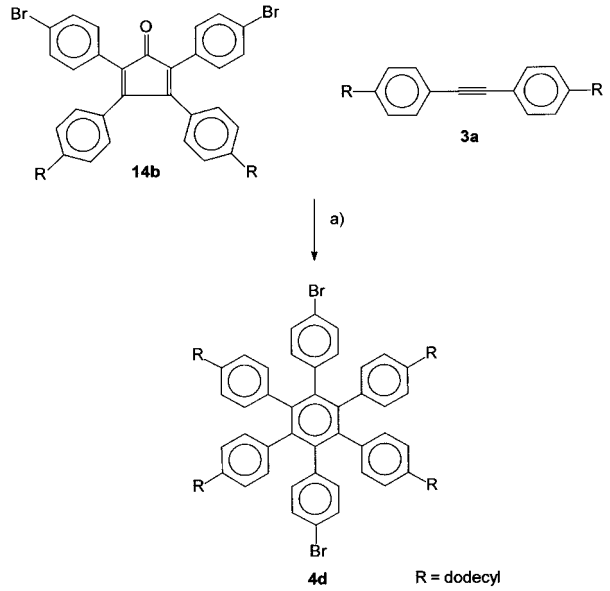

Scheme 6. Synthesis of bromo-substituted hexaphenylbenzene **4d**. a) Diphenylether, reflux (74%).

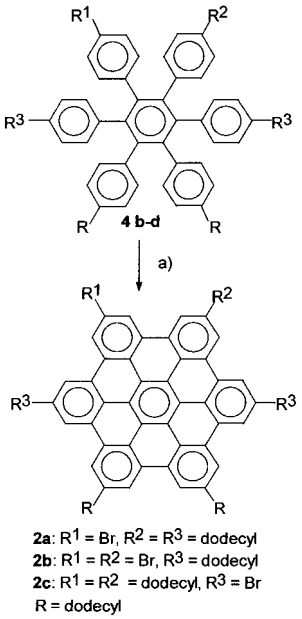

Scheme 7. Synthesis of bromo-substituted HBCs **2a–c**. a) $FeCl_3$, CH_3NO_2, CH_2Cl_2, RT (87–93%).

tives.[8] However, reaction of the bromo-substituted hexaphenylbenzenes **4b–d** under these oxidative conditions failed to yield the desired products. According to mass spectrometry, only partially cyclized products were formed. Also, treatment of the HBC-precursors under various other oxidative coupling conditions that had been developed by Kovacic[28] for the synthesis of poly-*para*-phenylenes from benzene did not lead to the desired HBC derivatives in high yields. Addition of iron(III)chloride to a solution of the precursor in dichloromethane,[29] led to unseparable mixtures of hexa-*peri*-hexabenzocoronene derivatives and chlorinated by-products. The formation of the undesired by-products could be successfully suppressed by dissolving the iron(III)chloride in nitromethane before adding it to the reaction mixture and by purging out HCl evolving during the reaction. Using these improved conditions (Scheme 7), products **2a–c** were isolated in excellent yield after quenching the reaction with methanol (90–95%).

We planned to introduce different electron donating and electron withdrawing substituents at the aromatic core using the monobromo-substituted HBC **2a**. Lithiation with *n*-butyllithium in tetrahydrofuran followed by quenching of the lithiated species with various electrophiles did not yield the desired products but resulted in the dehalogenated PAH in up to 80% yield. However, by using Pd-catalyzed coupling reactions, we were able to introduce various substituents (Scheme 8 and Scheme 9). It was possible to cross-couple primary and secondary amines with the monobromo-HBC **2a** under catalysis with $Pd_2(dba)_3$ and BINAP in the presence of sodium *tert*-butanolate.[30] With this method, we obtained undecylamino-HBCs **15a,b,c** and piperidino-HBC **16** in 80% yield (100% conversion).[31] By analogy to this reaction, we tried to synthesize ether derivatives by similar cross-coupling of alcohols and **2a** with the above mentioned catalyst system.[32] In contrast to the previous synthesis, the alcohols did not react at all or the conversion was very low. The

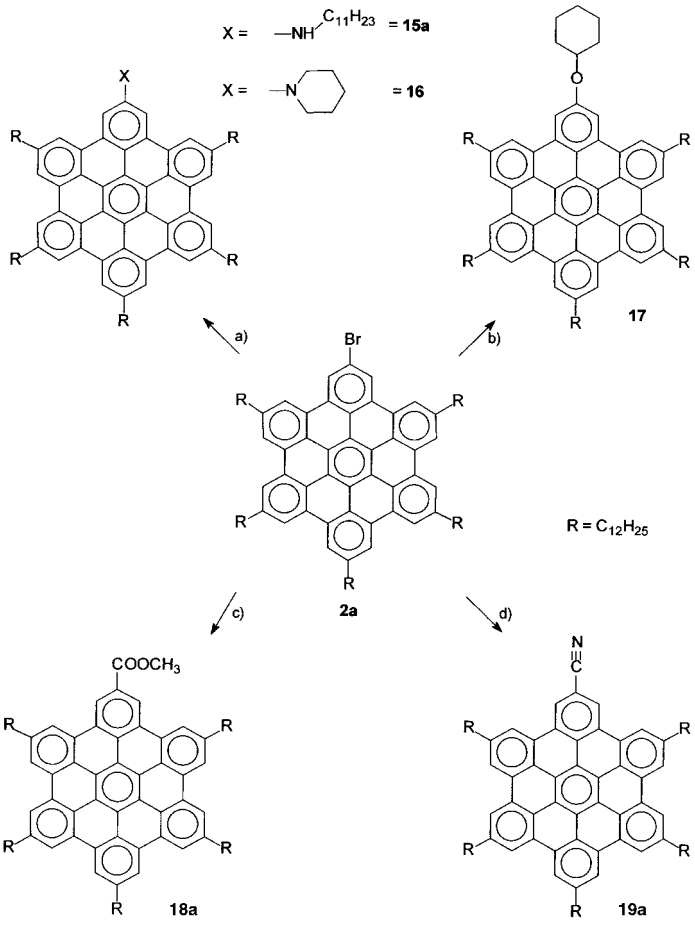

Scheme 8. Synthesis of mono functionalized HBC derivatives. a) **15a**: undecylamine, sodium *tert*-butoxide, (*R*)-BINAP, Pd^0, toluene, 80°C, 4 h (74%); **16**: piperidine, sodium *tert*-butoxide, (*R*)-BINAP, Pd^0, toluene, 80°C, 4 h (78%); b) cyclohexanol, NaH, (*R*)-BINAP, Pd^0, toluene, 80°C, 2 h (17%), c) CO, methanol, $Pd(PPh_3)_2$, PPh_3, triethylamine, THF, 100°C, 5 d (62%), d) CuCN, NMP, 195°C, 20 h (61%).

0947-6539/00/0623-4330 $ 17.50+.50/0 *Chem. Eur. J.* **2000**, *6*, No. 23

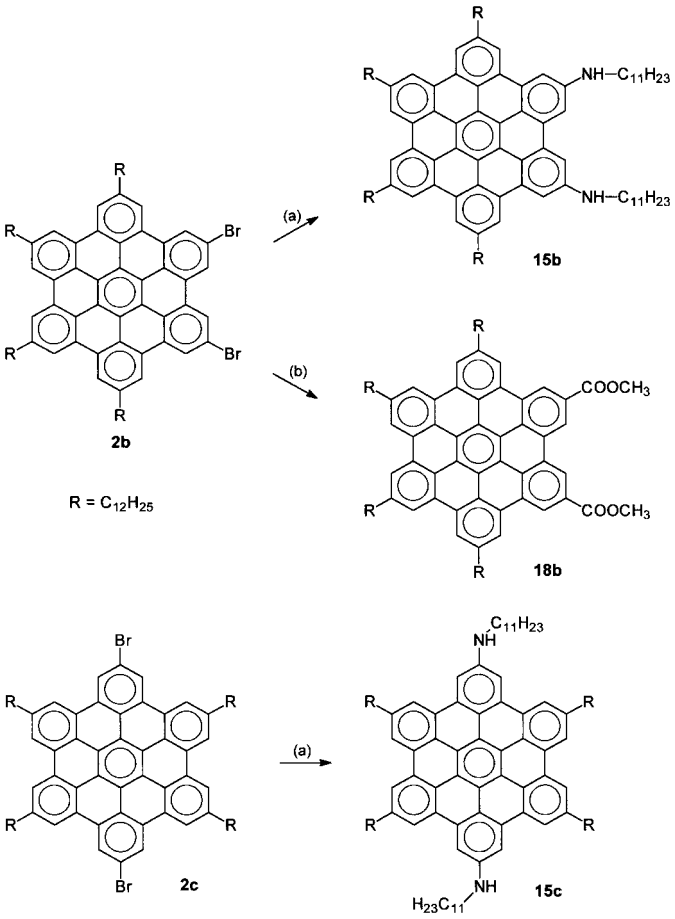

Scheme 9. Synthesis of bis-functionalized HBC derivatives. a) Undecylamine, sodium *tert*-butoxide, (*R*)-BINAP, Pd^0, toluene, 80 °C, 4 h (75 %); b) CO, methanol, $[Pd(PPh_3)_2Cl_2]$, PPh_3, triethylamine, THF, 100 °C, 5 d (62 %).

primary alcohol undecanol did not give the corresponding ether derivative but afforded the dehalogenated PAH in 78 % yield, whereas the secondary alcohol cyclohexanol cross-coupled with **2a** to give the cyclohexyl ether **17** in low yield (17 %). Besides these derivatives with electron donating substituents, it was also possible to introduce electron withdrawing substituents by a Pd-catalyzed reaction. In a Pd^{II} catalyzed carbonylation reaction with CO and methanol under high pressure,[33] the methyl esters **18a** and **18b** were synthesized in 60 % yield. With the cyano-HBC **19a**, another derivative with a strongly withdrawing substituent could be obtained in similar yield (61 %) by a Rosenmund–von Braun[34] reaction with CuCN in *N*-methylpyrrolidone.

All attempts to obtain analytically pure diester **18c** and the dicyano-HBCs **19b** and **19c**, applying the same reaction conditions as described above, were unsuccessful. Even though, the reactions yielded the desired products, it was not possible to separate them from the starting material and side products.

The new derivatives could be unambiguously characterized by NMR spectroscopy, mass spectrometry, IR spectroscopy, UV/Vis spectroscopy,[35] and elemental analysis. The NMR spectra show the expected number of signals, but the chemical shifts in the ^{1}H-NMR spectra are strongly concentration dependent as was observed for **1a** before (see Experimental Section). This is due to the strong $\pi-\pi$-interaction in aggregates which are present even at low concentrations.

Characterization of the mesophase behavior

The mesogenic properties of compounds **1**, **2**, and **15–19** were investigated using optical microscopy, DSC, and X-ray diffraction. A summary of the thermal behavior deduced from these techniques is shown in Tables 1, 2.

DSC Study: At room temperature all compounds are solids, but they exhibit a liquid crystalline phase at slightly elevated temperatures. Compounds **1**, **2**, **15a**, and **16–19** form a single mesophase over a broad temperature range. One strongly endothermic peak with a characteristic enthalpic value of about 40–50 J g^{-1} was observed during the heating cycle and assigned to the solid-to-mesophase transition. In some cases additional phase transitions could be identified at low temperatures by small enthalpy changes. These phases are, presumably, due to polymorphism in the crystalline or plastic crystalline state.

The transition from the mesophase into the isotropic liquid is accompanied by a small change in enthalpy of about 5 J g^{-1}, but was measured only exceptionally, since it occurs at temperatures above 400 °C, where decomposition slowly starts. At temperatures below 300 °C, where no decomposition was observed, compounds **1**, **2**, **15a**, and **16–19** exhibit reversible phase transitions.[36] However, these HBC derivatives show strong supercooling (up to 60 °C) and, in some cases, tend to recrystallize only partially.

The bis-amines **15b** and **15c** exhibit a slightly different phase behavior. Even though DSC shows only one phase transition into a mesophase, an additional phase was observed by X-ray diffraction for both bis-amines **15b** and **15c**. In case of **15c**, an approximately rectangular columnar phase was identified, which is stable between 95 and 115 °C. For compound **15b** a phase was observed which is only stable in a small temperature range around 90 °C before the transition into the hexagonal discotic mesophase occurs. This phase was repeatedly observed upon heating, but could not be detected upon cooling. The reason for the different phase behavior of compounds **15b** and **15c** compared with **1**, **2**, **15a**, or **16–19** is not yet well understood, but we expect that hydrogen bonding between NH groups, resulting in a stronger coupling of the disk-like molecules, plays a crucial role.

Optical microscopy study: To study the thermal behavior of the compounds **1**, **2**, and **15–19** by polarization microscopy a drop cast film was prepared from dichloromethane solution. Upon heating under nitrogen the compounds underwent a phase transition into a highly viscous phase, which exhibited a much stronger birefringence than the initial, partially crystalline material. The textures observed at temperatures up to about 230 °C were not characteristic of a particular superstructure, but upon further heating to a maximum of 420 °C growing domains with textures typical for a columnar mesophase[1, 37] were observed for many compounds without noticeable decomposition. Those textures did not change

Table 1. Optical, thermal, and thermodynamic data of compounds **1**, **2**, and **15**–**19** (C = crystal, LC = liquid crystal, Col_{ho} = ordered hexagonal columnar mesophase, I = isotropic liquid) for the second heating.

Compound	Transition	T [°C]	ΔH [J g^{-1}]
1b	C-Col_{ho}	106.5	60.6
	Col_{ho}-I	417	5.7
1d	C-Col_{ho}	124.4	50.8
	Col_{ho}-I	412[a]	
2a	C-Col_{ho}	74.1	46.6
	Col_{ho}-I	> 420[a]	
2b	C-Col_{ho}	59.3	40.7
	Col_{ho}-I	> 420[a]	
2c	C-Col_{ho}	104.3	79.1
	Col_{ho}-I	> 420[a,b]	
15a	C-Col_{ho}	89.4	40.1
	Col_{ho}-I	410 – 425[a]	
15b	C-LC	89.7	51.8
	LC-Col_{ho}	≈ 95[c]	
	Col_{ho}-I	> 420[a]	
15c	C-Col_{r}	95.6	44.9
	Col_{r}-Col_{ho}	≈ 115[c]	
	Col_{ho}-I	360 – 405[a]	
16	C-Col_{ho}	101.7	40.3
	Col_{ho}-I	> 420	
17	C-LC	95.9	39.2
	LC-I	404[a,b]	
18a	C-Col_{ho}	82.6	47.3
	Col_{ho}-I	> 420[a]	
18b	C-Col_{ho}	83.0	41.2
	Col_{ho}-I	380 – 400[a,b]	
19a	C-LC	77.3	31.5
	LC-I	> 420[a]	

[a] A transition observed by optical microscopy. [b] Decomposition noticeable during optical microscopy. [c] Transition observed by X-ray diffraction.

during cooling until the sample recrystallized, which could be observed as fracturing of the mesophase texture in some cases.

For those compounds (**1d**, **15a**, **15c**, **17**) with clearing points below 420 °C even fast cooling (15 K min^{-1}) of the optically isotropic liquid gave well-developed birefringent domains typical for columnar mesophases, but often only after pronounced supercooling of the optically isotropic liquid phase. The observed textures include ribbon- or fan-like as well as dendritic domains: Figure 4 shows some typical examples.

X-ray Diffraction study: The structure of the different phases of compounds **1**, **2**, and **15**–**19** were examined by temperature dependent X-ray diffraction. At temperatures up to the first highly endothermic phase transition the diffraction patterns, in combination with the mechanical behavior, indicated the presence of a crystalline phase, however, the alkyl chains were not well ordered in most cases.

Above the melting point, the X-ray diffraction patterns of all HBC derivatives described in this paper yielded a set of peaks which are characteristic of a hexagonal columnar mesophase (Figure 5).[8, 38] Three to five reflections are observed at low angles with the first one being much more intense than the other ones. Their reciprocal spacings follow the ratio $1:\sqrt{3}:\sqrt{4}:\sqrt{7}:\sqrt{9}$, and they can be indexed as 10-, 11-, 20-, 21-, and 30 reflections of a quasi two-dimensional hexagonal lattice with intercolumnar distances of about 26 to 31 Å. In addition to these reflections a broad halo with its center around 4.7 Å was observed, which is associated to the liquid-like correlation between aliphatic chains.[39] The 001-reflection at about 3.5 – 3.6 Å indicates the periodic stacking of the molecular cores in the columns.[40]

The liquid crystalline samples could be easily aligned by mechanical shearing, for example by extrusion to a fiber. In case of compounds **1c** and **2a**, the fibers recrystallized

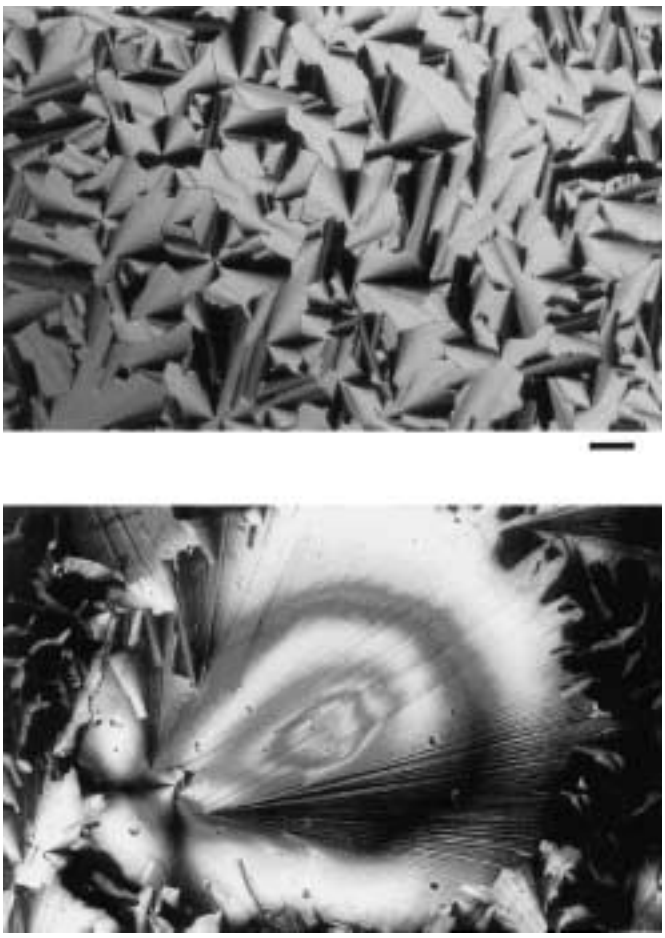

Figure 4. Optical textures of the hexagonal discotic mesophase of **1d** observed under polarized light (crossed polarizers). Top: 408 °C (heating). Bottom: 380 °C (cooling), scale = 100 μm.

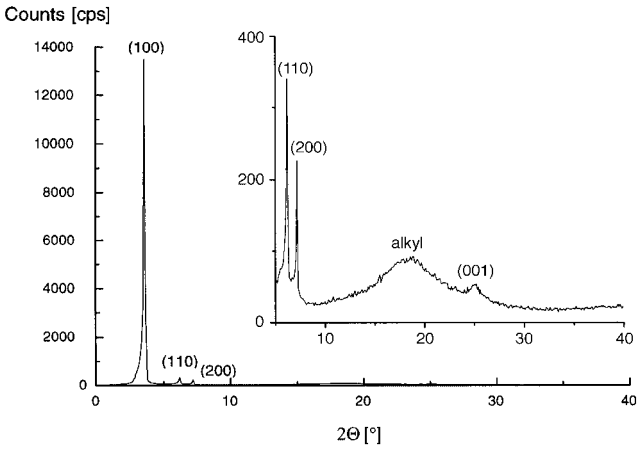

Figure 5. X-ray diffraction pattern of **2a** at 170 °C.

0947-6539/00/0623-4332 $ 17.50+.50/0 *Chem. Eur. J.* **2000**, *6*, No. 23

Table 2. Lattice spacings obtained by X-ray diffraction for the mesophase of compounds **1**, **2**, and **15**–**18** at 170 °C.

Compound	*h*	*k*	*l*	*d* [Å]	Lattice constant [Å]	Calcd density[a] [g cm^{-3}]		V_{CH_2} [Å^3][b]
1b	1	0	0	25.6	$a = 29.6$	Col_{ho}	0.95	31.8
	1	1	0	14.8				
	2	0	0	12.3				
	0	0	1	3.55	$c = 3.55$			
1c	1	0	0	26.7	$a = 30.7$	Col_{ho}	0.95	30.7
	1	1	0	15.3				
	2	0	0	13.3				
	0	0	1	3.67	$c = 3.67$			
1d	1	0	0	23.3	$a = 27.2$	Col_{ho}	0.99	31.7
	1	1	0	13.6				
	2	0	0	11.2				
	0	0	1	3.60	$c = 3.60$			
2a	1	0	0	24.5	$a = 28.3$	Col_{ho}	0.98	33.8
	1	1	0	14.2				
	2	0	0	12.3				
	0	0	1	3.54	$c = 3.54$			
2b	1	0	0	22.8	$a = 26.3$	Col_{ho}	1.07	34.5
	1	1	0	13.2				
	2	0	0	11.4				
	2	1	0	8.7				
	3	0	0	7.7				
	0	0	1	3.52	$c = 3.52$			
2c	1	0	0	22.7	$a = 26.2$	Col_{ho}	1.08	34.0
	1	1	0	13.1				
	2	0	0	11.4				
	0	0	1	3.51	$c = 3.51$			
15a	1	0	0	24.4	$a = 28.1$	Col_{ho}	1.02	29.1
	1	1	0	14.2				
	2	0	0	12.1				
	0	0	1		c =			
15b	1	0	0	24.9	$a = 28.7$	Col_{ho}	1.00	30.5
	1	1	0	14.4				
	2	0	0	12.5				
	0	0	1	3.62	$c = 3.62$			
15c	1	0	0	24.3	$a = 28.0$	Col_{ho}	1.03	29.3
	1	1	0	14.1				
	2	0	0	12.1				
	0	0	1	3.68	$c = 3.68$			
16	1	0	0	25.1	$a = 29.0$	Col_{ho}	0.94	32.7
	1	1	0	14.5				
	2	0	0	12.5				
	0	0	1	3.56	$c = 3.56$			
18a	1	0	0	24.7	$a = 28.6$	Col_{ho}	0.93	33.9
	1	1	0	14.4				
	2	0	0	12.4				
	3	0	0	8.3				
	0	0	1	3.59	$c = 3.59$			
18b[c]	1	0	0	24.0	$a = 27.7$	Col_{ho}	0.94	36.1
	1	1	0	13.7				
	2	0	0	12.0				
	0	0	1	3.51	$c = 3.51$			

[a] The density was calculated using the following Equation: $\rho = \frac{M/N}{V}$, with M = molecular weight, N = Avogadro number, $V = \frac{2}{\sqrt{3}} a^2 c$: volume unit cell. [b] V_{CH_2} was calculated by the following Equation $V_{CH_2} = \frac{V_{mol} - V_{core} - V_{subst}}{N_{CH_2}}$ with V_{mol} = unit cell volume, V_{core} = volume of HBC core (410 Å^3), and V_{subst} = volume of varying substituents (non CH_2), and N_{CH_2} = number of CH_2 and CH_3 groups. [c] X-ray diffraction measurements were done in a 2 mm capillary instead of a copper goniometer.

immediately upon cooling to room temperature, retaining the preferential orientation, but in case of the dibromo-substituted compound **2b** the hexagonal columnar mesophase was stable for more than three months at room temperature. The diffraction pattern of this fiber (Figure 6) proved the orientation of the columns to be along the fiber axis.

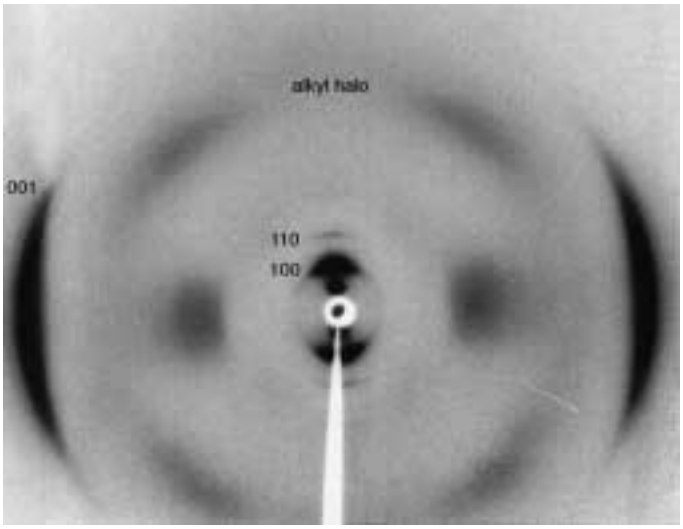

Figure 6. X-ray diffraction pattern of an extruded fiber of **2b** at room temperature (beam direction normal to fiber axis).

Figure 7 shows the X-ray diffraction pattern of compound **15c** at 110 °C. The first three reflections can be indexed in agreement with an approximately rectangular structure with $a = 33.7$ Å, but the split reflection at about 6.5° indicates a small distortion from a rectangular geometry. The reflection

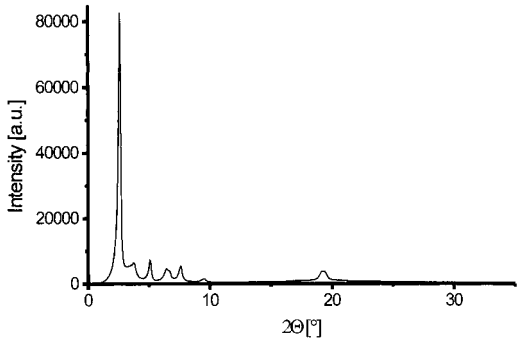

Figure 7. X-ray diffraction pattern of compound **15c** at 110 °C.

at 4.67 Å is indexed as a 001-reflection, indicating the stacking periodicity. Assuming a center-to-center distance of 3.6 Å, this corresponds to a tilt angle of about 40° for the molecular plane with respect to the column axis.

Scanning tunneling microscopy (STM): As mentioned in the introduction, different current-voltage characteristics through single alkylated HBC molecules of **1b** have been detected for the aromatic and aliphatic parts,[13] and it is expected that the functionalization of the aromatic core will influence the packing patterns and possibly the current voltage characteristics. The immobilization of the functionalized HBCs in two-dimensional molecular patterns and the submolecularly resolved scanning tunneling microscopy (STM) are also

prerequisites for the spectroscopy. Therefore, in situ STM measurements were carried out at the solid–fluid interface between an organic solution containing the functionalized HBCs (**1b**, **1d**, **2a**, and **15a–c**), and the atomically flat basal plane of highly oriented pyrolytic graphite (HOPG), following a strategy developed some time ago.[11, 41–45]

The present investigation is concerned with the influence of chemical modification on the two-dimensional crystal structure. In particular, how far will the replacement of an alkyl side chain by a hydrogen atom or a bromine atom or the insertion of amino groups into an alkyl chain modify the two-dimensional crystal structures? The electronic characterization of the molecules within the patterns shall be presented elsewhere.[46]

For hexaalkyl-substituted HBC **1b** two different molecular patterns could be observed (Figure 8a). Like in all STM images of the present paper the areas of higher tunneling current are attributed to the aromatic moiety of the molecules.[47–49] Besides a rhombic lattice, which has been already described for **1b**,[13] also a two-dimensional crystal structure is found, in which the molecules are dimerized. In Figure 8a two

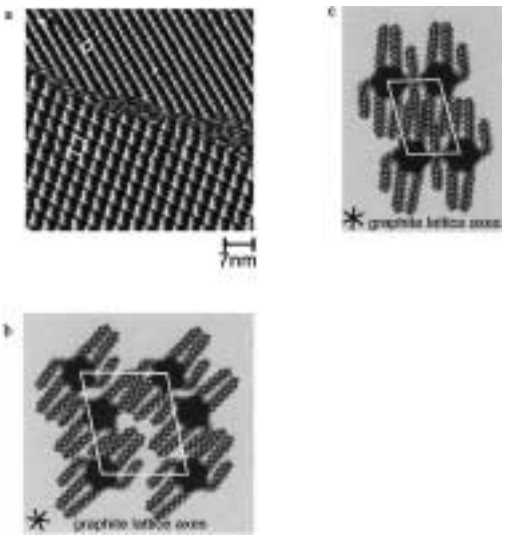

Figure 8. a) STM image (constant height mode) of the two-dimensional crystal structures of **1b**; b) packing model of the dimer row structure of **1b**; c) packing model of the rhombic lattice of **1b**.

domains are visible, which are separated by a wide domain boundary, where the molecules are disordered. The domain in the upper part of the STM image exhibits the rhombic lattice, while in the domain in the lower part of the image the dimer row structure is observed. The lattice constants of both crystalline structures are given in Table 3.

The parallel orientation of all alkyl side chains along a substrate lattice axis leads to a closely packed crystal. From the comparison of Figure 8a with the STM images revealing the underlying graphite lattice (not displayed) one can determine, which axes of both two-dimensional lattices correspond to graphite axes. Packing models have been constructed and displayed in Figure 8b,c. The short diagonal of the unit cell of the dimer row structure corresponds to a graphite lattice axis, while there is no correspondence between the axes of the rhombic lattice (determined by the positions of the aromatic cores) and the graphite substrate.

Table 3. Lattice constants of all described two-dimensional crystal structures of functionalized HBC.

	Lattice type	Lattice parameters	Area per molecule in nm^2
1b	dimer rows	$a = 3.40 \pm 0.17$ nm $b = 4.02 \pm 0.21$ nm $\alpha = 76^\circ \pm 2^\circ$ $x = 1.64 \pm 0.17$ nm $\beta = 61^\circ \pm 4^\circ$	6.63 ± 0.75
	rhombic	$a = 1.88 \pm 0.09$ nm $b = 2.68 \pm 0.11$ nm $\alpha = 80^\circ \pm 2^\circ$	4.96 ± 0.48
1d	dimer rows	$a = 2.89 \pm 0.11$ nm $b = 4.56 \pm 0.08$ nm $\alpha = 72^\circ \pm 3^\circ$ $x = 1.84 \pm 0.16$ nm $\beta = 61^\circ \pm 2^\circ$	6.27 ± 0.45
	rhombic	$a = 1.86 \pm 0.07$ nm $b = 2.60 \pm 0.08$ nm $\alpha = 79^\circ \pm 3^\circ$	4.75 ± 0.37
15a	dimer rows	$a = 2.98 \pm 0.06$ nm $b = 4.29 \pm 0.08$ nm $\alpha = 75^\circ \pm 2^\circ$ $x = 1.83 \pm 0.14$ nm $\beta = 63^\circ \pm 5^\circ$	6.17 ± 0.30
15b	dimer rows	$a = 2.89 \pm 0.15$ nm $b = 4.36 \pm 0.37$ nm $\alpha = 76^\circ \pm 4^\circ$ $x = 1.70 \pm 0.16$ nm $\beta = 66^\circ \pm 4^\circ$	6.11 ± 0.97
15c	dimer rows	$a = 2.94 \pm 0.08$ nm $b = 4.39 \pm 0.23$ nm $\alpha = 71^\circ \pm 2^\circ$ $x = 1.82 \pm 0.21$ nm $\beta = 56^\circ \pm 4^\circ$	6.10 ± 0.57
2a	hexagonal	$a = b = 6.41 \pm 0.16$ nm $\alpha = 60^\circ \pm 2.5^\circ$ $c = 2.70 \pm 0.16$ nm $\beta = 29^\circ \pm 1^\circ$ $p = 5.72 \pm 0.15$ nm $g = 2.75 \pm 0.12$ nm $x = 1.64 \pm 0.95$ nm	5.07 ± 0.39

For pentaalkyl-substituted HBC **1d** also two molecular patterns could be observed: A dimer row structure (Figure 9a, Table 3) and a rhombic lattice (Figure 9c, Table 3). Similarly to the case of **1b**, discussed above, packing models have been constructed, which are shown in Figure 9b (dimer rows) and Figure 9d (rhombic lattice). Obviously, the symmetries of both structures are identical to the ones reported for **1b**.

By introducing amino groups one may expect changes of the molecular arrangement due to hydrogen bonds between neighboring molecules. The STM image of **15a** (Figure 10a) reveals dimer rows.

The average area per molecule (6.17 nm$^2 \pm 0.30$ nm^2, see Table 3) is a little larger than the calculated value[50] (5.69 nm^2). From the experiment, the short diagonal of the unit cell corresponds to a graphite lattice axis. Therefore, one may expect that all alkyl chains are aligned along this axis (Figure 10b). Moreover, Figure 10b demonstrates that distances between the amino groups of neighboring molecules are too large for intermolecular hydrogen bonds. On the other

0947-6539/00/0623-4334 $ 17.50+.50/0 *Chem. Eur. J.* **2000**, *6*, No. 23

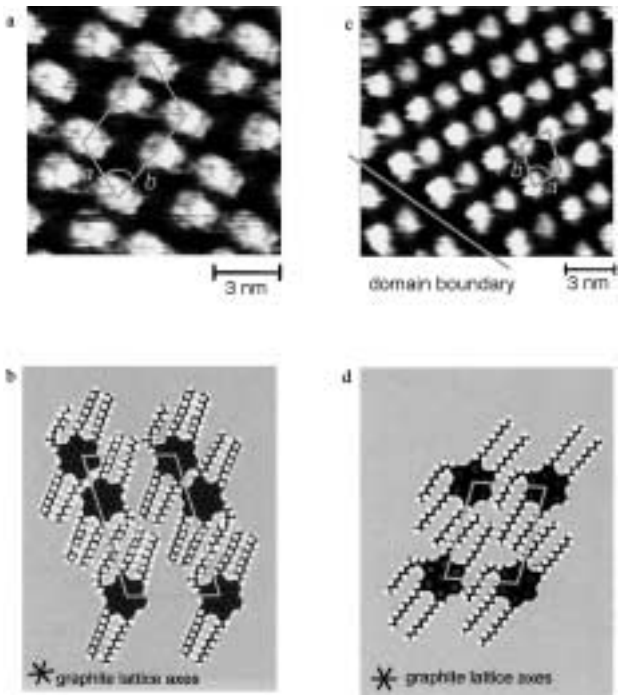

Figure 9. a) STM image (constant current mode) of the dimer row structure of **1d**; b) packing model of the dimer row structure of **1d**; c) STM image (constant current mode) of the rhombic lattice of **1d**; d) packing model of the rhombic lattice of **1d**.

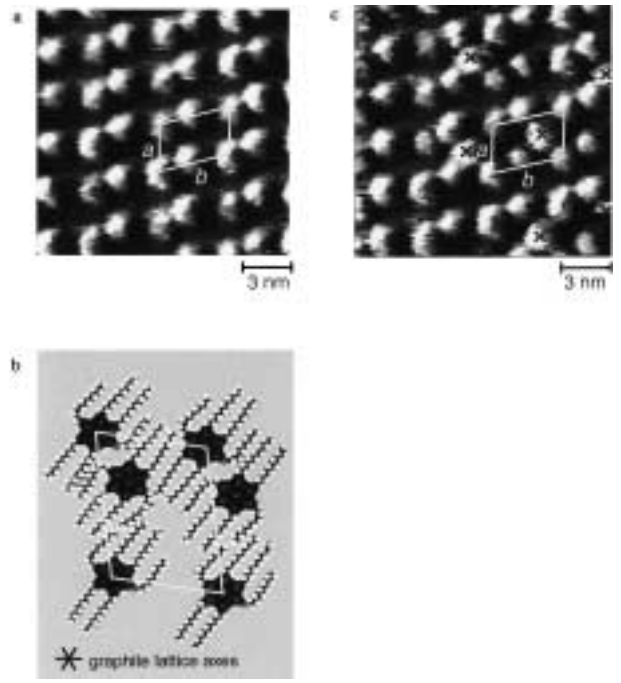

Figure 10. a) STM image (constant height mode) of the dimer row structure of **15a**; b) packing model of the dimer row structure of **15a**; c) STM image (constant height mode) of the dimer row structure of **15a**, with interstitials (marked with x).

hand, hydrogen bonds cannot be completely excluded, given the error of the unit cell data.

The described lattice of dimer rows is the only molecular pattern observed for **15a**. Often additional molecules are located between the dimer rows in interstitial positions. Figure 10c shows quite a high number of these interstitial molecules.

No change of the lattice constants was observed caused by the additional molecules, but locally a closer packing is obtained. The calculated value for a closely packed crystal indicates that alkyl chains have to be lifted out of the crystalline interfacial monolayer into the organic solution; otherwise, within the monolayer there would be not enough empty space for interstitial molecules. The analysis of all measured STM images indicates that the additional incorporation of molecules does not initiate a phase transition to a more closely packed crystal structure, but rather the interstitials are filled statistically. The already known dimer row structure is also the typical two-dimensional lattice for **15b** and **15c** (Table 3).

The symmetries of the two-dimensional crystals of the functionalized HBCs reported so far are the same as for the fully alkylated HBC. A different case is a bromo-substituted HBC **2a**. Figure 11 shows the STM image of **2a**, which is a

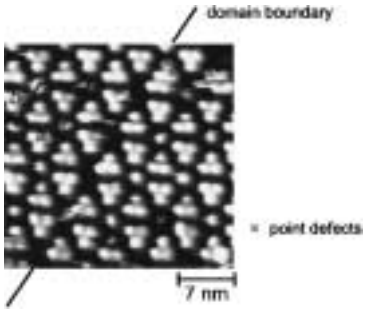

Figure 11. STM image (constant current mode) of the hexagonal lattice of **2a**.

rather complex two-dimensional lattice structure. The lattice contains two types of molecules: molecules associated in trimers and single molecules. The orientation of neighboring trimers alternates.

Single molecules and trimers assemble in a supramolecular pattern. A hexagonal lattice results (Table 3), in which single molecules fill positions in the center of an ensemble of six trimers, while every trimer is surrounded by three single molecules.

The positions of the bromine atoms within the two-dimensional crystal structure of **2a** could not be resolved. As it has been often observed for crystals of other chloro-, bromo-, and iodo derivatives,[51–55] halogen end groups tend to be adjacent to each other. For that reason, it seems to be most probable that within the two-dimensional lattice of **2a** bromine atoms are located in the center of trimers (see Discussion).

Discussion

It appears that mono- and dibromo derivatives of HBC **2a,b,c** are readily available via the Diels–Alder synthesis of adequately substituted hexaphenylbenzenes and their subsequent cyclodehydrogenation. The chemical transformation of the bromo substituted HBC derivatives is limited for several

reasons. The molecules are unstable under highly acidic conditions and show a relatively low solubility in organic solvents at room temperature. This is especially true for the dibromo compound **2c**, which has an even lower solubility than **2a** or **2b**. Further problems arise in the purification process of these extremely large polycyclic aromatic hydrocarbons. It is often not possible to separate different HBC derivatives on a chromatography column or to get analytically pure samples by recrystallization, due to the long alkyl tails. Therefore, it is necessary to have clean reactions with a high conversion, especially in case of dibromo-HBCs **2b** and **2c**. The synthesis of **15**, **18**, and **19** may serve as typical examples. It is possible to react the "superbenzene" HBC-molecule under various conditions known from benzene chemistry. In contrast to phthalocyanines, where selectively functionalized derivatives are hard to obtain, the HBCs allow a direct correlation of the varying substitution pattern with the packing behavior and the electronic properties.

X-ray diffraction of all HBC derivatives described herein reveals the formation of hexagonal columnar mesophases with the exception of **15c** which exhibits an approximately rectangular structure. The density of the substituted HBCs, calculated from the X-ray diffraction data, is typically on the order of $0.95-1.0\ g\,cm^{-3}$ as is expected for these kinds of compounds. Only compounds **2b** and **2c** have a higher density of about $1.07\ g\,cm^{-3}$, presumably due to the heavy bromo substituents. The calculated volume of a CH_2 group is on average 31.4 Å^3 for the pure hydrocarbons, a relatively large, but still typical value in discotic mesophases.[56, 57] On substituting the alkyl chains by a short but bulky group (e.g., bromo or methylester) the calculated volume per CH_2 group increases to about 33–35 Å^3 with this effect being most pronounced for the *ortho* disubstituted hexa-*peri*-hexabenzocoronene derivatives. One explanation for this observation is the flexibility of the alkyl chains which does not allow the complete filling of the space around the bulky substituents, thus leaving a small free volume in the periphery of these groups.

We conclude that the different substituents in HBC derivatives induce only small differences in the mesophase structure and stability. This is in contrast to observations made for triphenylenes where the mesophase stability is very sensitive towards different substituents or substitution patterns.[58] An explanation for the different properties of substituted HBCs compared with triphenylenes is the stronger $\pi-\pi$ interaction and the larger size of the aromatic core in case of HBC, which stabilizes the mesophase dramatically and allows for the incorporation of different substituents without losing mesomorphic properties.

While transitions from parent HBCs **1a,b,c** to their chemically functionalized analogues does not cause significant changes of the liquid crystalline phases, STM studies reveal profound changes of the resulting monomolecular adsorbate layers on HOPG surfaces. It is of key importance to carefully follow the relation between molecular structures and their two-dimensional patterns on substrates which may serve as anchoring layers in devices. While organic chemistry has accumulated a vast number of three-dimensional crystal structures, the study of two-dimensional crystals is still in its infancy.

It becomes obvious from the STM image of hexaalkyl HBC **1b** that the alkyl side chains are located in the area of lower tunneling current. As with all other STM images presented in this paper, they could not be molecularly resolved, indicating a high conformational mobility at room temperature. However, on graphite the alkyl side chains tend to align along a substrate lattice axis, as already described for many other alkylated molecules studied with STM.[11, 14, 59]

Noteworthy, the dimer row structure (Figure 8b) reveals empty space in the two-dimensional arrangement of the molecules of **1b**. Correspondingly, the area per molecule determined by the STM experiment ($A_{dr} = 6.63\ nm^2 \pm 0.75\ nm^2$) is significantly larger than the calculated value for closely packed molecules ($A_{theor} = 5.67\ nm^2$) given by the van der Waals contour of the flat lying molecules.[50] The empty space is presumably filled with solvent. The rhombic lattice (Figure 8c) on the other hand, is closely packed ($A_{rh} = 4.96\ nm^2 \pm 0.48\ nm^2$). Since crystals generally tend to be closely packed, the average area per molecule may be used as a means to estimate the relative stability of both crystals: The denser packing of molecules within the rhombic lattice indicates its higher stability.[60] Thus, it is not surprising that with time the denser and more stable rhombic lattice is the favored two-dimensional crystal structure of **1b** molecules.

The dimer row structure and rhombic lattice of **1d** were found to coexist for a long time (Figures 9a–d). Unfortunately, the phase transition between both crystal structures could not be observed in situ in the STM, probably because of the limited measuring time.[61] The area which one **1d** flat lying molecule needs within the rhombic lattice ($A_{rh} = 4.75\ nm^2 \pm 0.37\ nm^2$), differs substantially from the dimer row case ($A_{dr} = 6.27\ nm^2 \pm 0.45\ nm^2$). The theoretical value for closely packed molecules of **1d** ($A_{theor} = 4.99\ nm^2$), as calculated from the van der Waals contour of flat flying molecules,[50] fits well with A_{rh}. Thus, the rhombic lattice structure has to be considered as the most stable crystalline modification of **1d** (as already demonstrated for **1b**). Based on this assumption the less closely packed dimer row structure may be a metastable preadsorbate.

The crystal symmetries of **1d** are unchanged in comparison with those of **1b**. This is not obvious, since the symmetry of the free molecules is reduced by the chemical modification, and new crystal symmetries might be anticipated. The absence of additional intermolecular forces may explain why the substitution of an alkyl chain by a simple hydrogen atom does not entail any significant changes of crystal symmetry. The present investigation of crystal structures of **1b** and **1d** indicates that stronger chemical modifications are necessary to assemble different stable molecular patterns.

The insertion of NH functionality into the alkyl chains leads to a stabilization of the dimer row structure when comparing compounds **15** and **1b**. The failure to observe a different packing when varying both number and position of functional groups indicates that the two-dimensional crystal symmetry is probably more determined by requirements of dense packing than by additional intermolecular forces such as, for example hydrogen bonding.

A completely different situation is encountered for the monolayer of the bromo-substituted HBC **2a** because one

  0947-6539/00/0623-4336 $ 17.50+.50/0 *Chem. Eur. J.* **2000**, *6*, No. 23

visualizes patterns coexisting of both trimeric assemblies and single molecules. The proximity of bromo end groups and the formation of trimers could be caused by attractive interactions[62–65] between bromine atoms of neighboring molecules. Close intermolecular contacts between more than two halogen groups as described in the present case for **2a** have been reported for many crystals,[54, 62, 66, 67] and triangular arrangements of halogen end groups are known, for example for 1,4-dichloro-benzene.[67] In general, two types of attractive interactions may be considered. Dispersion forces[62] can be responsible for the formation of crystalline structures where the halogen atoms (except fluorine)[55] are close to each other. In this case the intermolecular distances are determined by the sum of van der Waals radii of interacting atoms. The reason for halogen–halogen intermolecular contacts, which are shorter than expected from the van der Waals radius, has been controversially discussed in the literature. Price[62] and Nyburg[63] explain the decreased intermolecular distances between halogen end groups by an anisotropic model for the repulsion term. However, Desiraju[64] and Parthasarathy[65] conclude from angle preferences of intermolecular forces around halogen atoms that specific attractive interactions exist, which have been interpreted, for example as "donor–acceptor" interactions, "charge-transfer" interactions or "incipient electrophilic and nucleophilic attack". Assuming in a model treatment of the triangular arrangement of **2a** that the bromine atoms point toward the trimer center one estimates a distance of the aromatic cores of 1.64 nm. This distance agrees very well with the experimental value of $1.6\,\mathrm{nm} \pm 0.1\,\mathrm{nm}$. However, owing to the considerable error of the calculated distance one cannot decide on whether the distances are shorter than van der Waals type contacts (reduced van der Waals radii by 20% are within the error).

Conclusion

We have presented a new method to synthesize unsymmetrically substituted hexa-*peri*-hexabenzocoronenes by oxidative cyclodehydrogenation of suitable hexaphenylbenzene derivatives with iron(III)chloride in nitromethane, which tolerates bromine functions at the aromatic core. These bromo groups enable benzene-like substitution reactions for hexabenzocoronene, even though the reactions are limited due to the solubility of the HBC and the more demanding purification from similar by-products. Nevertheless, we were able to synthesize HBCs with several electron donating or electron withdrawing groups (Scheme 8 and 9).

These new hexa-*peri*-hexabenzocoronene derivatives self-assemble in the bulk as well as at the solid–fluid interface between an organic solution and HOPG. In situ scanning tunneling microscopy shows the influence of the substituents on the molecular packing in a two-dimensional crystal. Interestingly, the molecular symmetry is not determining the packing pattern. The hexaalkyl HBC **1b** exhibits the same two typical motives as the pentaalkyl HBC **1d**, namely a rhombic and a "dimer row" structure. Introducing a bromo function at the aromatic core causes a completely different packing pattern. The bromine groups of different molecules seem to interact strongly and thereby induce a hexagonal superstructure of six trimers and a single molecule. A similar superstructure could not be observed in the bulk mesophase.

The mesophases of the HBC derivatives are very stable with respect to variation of the substitution pattern. At high temperatures an ordered hexagonal columnar mesophase is observed. This might be due to the high temperature necessary for reaching the mesophase, which induces a high mobility of the molecules that competes with specific intermolecular forces such as the bromine–bromine interaction. On the other hand, the change from two-dimensional to three-dimensional may also be important bringing additional intermolecular forces into play. Noteworthy, while the amino groups in **15** induce only a slightly changed packing behavior in the two-dimensional crystals, these compounds were the only ones exhibiting an additional mesophase structure below the transition to the hexagonal columnar phase. We attribute this to hydrogen bonding between NH groups in the bulk mesophase.

In summary, the work presented proves the feasibility of "HBC-chemistry". The structural characterization gives first indications how the substitution of the aromatic core affects two-dimensional and three-dimensional ordering. Furthermore, gathering knowledge on the formation of monomolecular adsorbate layers and, in particular, correlating molecular structure and the packing mode in two-dimensional crystals are important steps toward molecular electronics. Subsequent studies by scanning tunneling spectroscopy can then detect an influence on the current voltage curve of the aromatic core upon a change of its electron density.

Experimental Section

STM procedure

In situ STM images were obtained at the interface between the basal plane of highly oriented pyrolytic graphite (HOPG, Union Carbide, quality ZYB) and a diluted solution of the functionalized HBCs in 1,2,4-trichlorobenzene ($c = 10^{-4}\,\mathrm{mol\,l^{-1}}$), following an experimental procedure reported elsewhere.[11, 41] Experiments were performed at room temperature with an in-house built microscope, which is based on the "Beetle" type STM[68, 69] and Omicron controls (CPU-3CE, SPM software version 2.1). Both electrochemically etched (2N KOH+6N KCN) and mechanically cut Pt/Ir (80:20) tips were used. Typical operation conditions for imaging the graphite lattice were negative sample bias (30–200 mV), tunneling currents around 0.2 nA and scan rates of 30 Hz per line.

First, STM images of the freshly cleaved substrate in pure solvent or air were recorded in "constant height" mode to calibrate the scanner for the currently used tip. Afterwards a drop of the organic solution containing the HBC was deposited on the graphite surface. Often spontaneous crystallization was observed; otherwise the crystallization was induced by an external voltage pulse between sample and tip (−(2–4) V). The two-dimensional crystals of physisorbed molecules were studied in the "constant current mode" as well as in the "constant height mode" under ambient conditions (negative sample bias: 1.0–1.8 V, tunneling current: 0.1–0.6 nA, scan rates: 30 Hz per line). After imaging of the molecular pattern the bias voltage was reduced to 30–200 mV, which allows to characterize the underlying graphite lattice.[45, 70] Based on this method one may determine the relative orientation between adsorbate and substrate lattices.

General methods

^{1}H-NMR and ^{13}C-NMR spectra were recorded in $CDCl_3$, $CDCl_3/CS_2$ 1:1, and $C_2D_2Cl_4$ on a Varian Gemini 200, Bruker DPX 250, Bruker AMX300,

and Bruker DRX500 with use of the solvent proton or carbon signal as internal standard. Melting points were determined on a Büchi hot stage apparatus and are uncorrected. Infrared spectra were recorded on a Nicolet FT-IR 320 spectrophotometer as KBr pellets. Mass spectra were obtained on a VG Instruments ZAB 2-SE-FPD by using FD. Elemental analysis were carried out on a Foss Heraeus Vario EL.

Differential scanning calorimetry (DSC) was measured on a Mettler DSC 30 with heating and cooling rates of 5–10 °C min^{-1}. First order transition temperatures were reported as the minima of their endothermic peaks during heating. A Zeiss Axiophot with a nitrogen flushed Linkam THM 600 hot stage was used to characterize the polarization microscopy textures and to estimate clearing temperatures. Heating and cooling rates varied between 5 and 20 °C min^{-1}.

X-ray diffraction experiments were performed using a Siemens D 500 Kristalloflex with a graphite-monochromatized $Cu_{K\alpha}$ X-ray beam, emitted from a rotating Rigaku RV-300 anode. The temperature of the samples, which were directly on a copper sample-holder or in glass capillaries, was measured by a bimetal sensor and calibrated by reference measurements.

Materials

$NiCl_2$(dppp), 1M dodecylmagnesiumbromide in diethyl ether, $AlCl_3$ (99%), dodecanoyl chloride (98%), hydrazine hydrate (98%), piperidine (99%), trimethylsilylacetylene (98%), KF (99%), 4-bromoiodobenzene (98%), sodium hydride (95%), iron pentacarbonyl, diphenyl ether (99%), nitromethane (96+%), undecylamine (98%), copper cyanide (99%), cyclohexanol (99%), and *N*-methyl-2-pyrrolidinone (99+%) (all from Aldrich) were used as received. Triphenylphosphine (97%), iodine (99.5%), CS_2 (99+%), dimethylformamide, benzyltriethylammoniumchloride (98%), and potassium-*tert*-butanolate (all from Fluka) were used as received. Iron(III)chloride (98%), triethylamine (99%), and copper iodide (98%) (all from Merck) were used as received. Trans-dichlorobis(triphenylphosphine)palladium(II) (99%), tris(dibenzylideneacetone)-dipalladium(**0**), and (*R*)-BINAP (98%) (all from Strem) were used as received. Dimethyl sulfoxide, methanol, ethanol, and chloroform (A.C.S. reagent, Riedel-de Haën) were used as received. THF (A.C.S. reagent, Riedel-de Haën) was refluxed over potassium and distilled freshly before use. Toluene (A.C.S. reagent, Riedel-de Haën) was refluxed over sodium and distilled freshly before use, CH_2Cl_2 (A.C.S. reagent, Riedel-de Haën) was dried over CaH_2 and freshly distilled before use.

Synthesis

4,4′-Didodecyl-*trans*-stilbene (5b): Dodecylmagnesiumbromide (550 mL, 1M in diethyl ether, 0.55 mol) was added to a solution of 4,4′-dibromo-*trans*-stilbene[18] (85 g, 251 mmol) and $NiCl_2$(dppp) (5.49 g) in diethyl ether (600 mL). After stirring overnight, 2M aqueous HCl was added to the reaction mixture. The organic phase, together with some precipitate was separated from the aqueous phase and the solvent was removed under reduced pressure. The residue was dissolved in dichloromethane and filtered over silica gel to afford 4,4′-didodecyl-*trans*-stilbene as a colorless solid (119 g, 92%): M.p. 80–82 °C; ^{1}H NMR (300 MHz, $CDCl_3$): $\delta = 7.43$ (d, $J = 8.0$ Hz, 4H), 7.18 (d, $J = 8.0$ Hz, 4H), 7.05 (s, 2H), 2.60 (t, $J = 7.6$ Hz, 4H), 1.1–1.8 (m, 40H), 0.90 (d, $J = 7.6$ Hz, 6H); ^{13}C NMR (75 MHz, $CDCl_3$): $\delta = 142.8$, 135.4, 129.1, 128.1, 126.7, 36.1, 32.3, 31.8, 30.1, 30.0, 29.9, 29.7, 23.1, 14.5; FD-MS: *m*/*z* (%): 516.4 $[M]^+$ (100); anal. calcd (%) for $C_{38}H_{60}$: C 88.30, H 11.70; found: C 87.91, H 11.43.

1,2-Dibromo-1,2-bis(4-dodecylphenyl)ethane (6): Bromine (6.7 mL, 131 mmol) was added to a solution of **5b** (68 g, 131 mmol) in chloroform (800 mL). After stirring overnight the solution was washed with aqueous sodium sulfite and water (2×) and dried ($MgSO_4$). The solvent was evaporated to afford **6** as a colorless solid (81 g, 90%): M.p. 115–117 °C; ^{1}H NMR (300 MHz, $CDCl_3$): $\delta = 7.50$ (d, $J = 8.0$ Hz, 4H), 7.25 (d, $J = 8.0$ Hz, 4H), 7.10 (d, $J = 8.0$ Hz, 4H), 7.00 (d, $J = 8.0$ Hz, 4H), 5.55 (s, 2H), 5.50 (s, 2H), 2.70 (t, $J = 7.8$ Hz, 4H), 2.55 (t, $J = 7.8$ Hz, 4H), 1.2–1.9 (m, 40H), 0.95 (d, $J = 7.6$ Hz, 6H); ^{13}C NMR (75 MHz, $CDCl_3$): $\delta = 144.4$, 143.8, 137.8, 135.5, 129.1, 128.9, 128.5, 128.1, 59.9, 56.8, 36.1, 35.9, 32.3, 31.6, 31.5, 30.1, 30.0, 29.9, 29.8, 29.6, 23.1, 14.5; FD-MS: *m*/*z* (%): 676.7 $[M]^+$ (100); anal. calcd (%) for $C_{38}H_{60}Br_2$: C 67.45, H 8.94; found: C 67.62, H 8.68.

4,4′-Didodecyldiphenylacetylene (3a): A solution of **6** (80 g, 118 mmol) and potassium-*tert*-butanolate (140 g, 1.248 mol) in *tert*-butanol (1 L) was heated at reflux overnight. The reaction mixture had cooled to room temperature and extracted with methyl-*tert*-butyl ether. The organic phase was washed with 2M aqueous HCl and a saturated sodium bicarbonate solution and dried ($MgSO_4$). After evaporation of the solvent the crude product was recrystallized from toluene to afford 4,4′-didodecyldiphenylacetylene (55 g, 69%): M.p. 58 °C; ^{1}H NMR (300 MHz, $CDCl_3$): $\delta = 7.40$ (d, $J = 8.4$ Hz, 4H), 7.12 (d, $J = 8.4$ Hz, 4H), 2.58 (t, $J = 7.2$ Hz, 4H), 1.6–1.2 (m, 40H), 0.86 (d, $J = 7.6$ Hz, 6H); ^{13}C NMR (75 MHz, $CDCl_3$): $\delta = 143.6$, 131.8, 128.8, 121.0, 89.3, 36.3, 36.2, 31.6, 30.0, 29.8, 29.8, 29.7, 29.6, 23.1, 14.5; FD-MS: *m*/*z* (%): 514.6 $[M]^+$ (100); anal. calcd (%) for $C_{38}H_{58}$: C 88.65, H 11.35; found: C 88.51, H 11.33.

4-Bromododecanoylbenzene: Dodecanoyl chloride (219 g, 1 mol) was added dropwise to a solution of bromobenzene (314 g, 2 mol) and aluminum chloride (160 g, 1.2 mol). The mixture was stirred at 50 °C for 1 h. The reaction mixture was then poured into ice water and extracted with dichloromethane. The organic phase was washed with 2M HCl and brine and dried (MgSO4). After removal of the solvent, the residue was purified by recrystallization from ethanol to afford 4-bromododecanoylbenzene as colorless plates (227 g, 67%): M.p. 64.0 °C; ^{1}H NMR (300 MHz, $CDCl_3$): $\delta = 7.73$ (d, $J = 8.0$ Hz, 2H), 7.52 (d, $J = 8.0$ Hz, 2H), 2.83 (t, $J = 7.5$ Hz, 2H), 1.63 (q, $J = 7.5$ Hz, 2H), 1.31–1.08 (m, 16H), 0.89 (t, $J = 7.0$ Hz, 3H); ^{13}C NMR (75 MHz, $CDCl_3$): $\delta = 199.86$, 136.21, 132.24, 129.99, 128.36, 38.98, 32.29, 30.00, 29.87, 29.85, 29.71, 24.68, 23.07, 14.49; FD-MS: *m*/*z* (%): 338.5 $[M]^+$ (100); anal. calcd (%) for $C_{18}H_{27}OBr$: C 63.72, H 8.02; found: C 63.46, H 7.96.

4-Bromododecylbenzene (7): A mixture of 4-bromododecanoylbenzene (200 g, 589 mmol), hydrazine hydrate (98%, 85.8 mL), and potassium hydroxide (132 g, 2.36 mol) in triethylene glycol (1 L) was heated at reflux for 2 h. The mixture was distilled at atmospheric pressure until the temperature of the reaction mixture reached 210 °C. After cooling to room temperature, the resulting mixture was poured into water, acidified with conc. HCl (220 mL), and extracted with dichloromethane. The organic phase was washed with water, dried ($MgSO_4$) and concentrated under reduced pressure. The residue was purified by column chromatography on silica gel with petroleum ether to afford **7** as colorless oil (130 g, 68%): ^{1}H NMR (300 MHz, $CDCl_3$): $\delta = 7.40$ (d, $J = 8.0$ Hz, 2H), 7.06 (d, $J = 8.0$ Hz, 2H), 2.58 (t, $J = 7.5$ Hz, 2H), 1.61 (quint, $J = 7.5$ Hz, 2H), 1.36–1.18 (m, 18H), 0.92 (t, $J = 7.0$ Hz, 3H); ^{13}C NMR (75 MHz, $CDCl_3$): $\delta = 142.25$, 131.65, 130.56, 119.64, 35.76, 32.33, 31.72, 30.05, 29.98, 29.87, 29.76, 29.60, 23.10, 14.51; FD-MS: *m*/*z* (%): 324.2 $[M]^+$ (100).

4-[(Trimethylsilyl)ethynyl]dodecylbenzene (8): A solution of **7** (20.3 g, 62.5 mmol), triphenylphosphine (1.65 g, 6.30 mmol), copper iodide (1.15 g, 6.02 mmol), and *trans*-dichlorobis(triphenylphosphine)palladium(II) (2.10 g, 3.00 mmol) in piperidine (400 mL) was heated at 50 °C and trimethylsilylacetylene (18 mL, 12.5 g, 127 mmol) was added dropwise. The resulting mixture was stirred at 80 °C for 24 h under an argon atmosphere. The reaction mixture was poured into a saturated NH_4Cl solution and extracted with dichloromethane. The organic phase was washed with half-saturated ammonium chloride solution and water. After removing the solvent the residue was purified by column chromatography on silica gel with petroleum ether to afford **8** (19.1 g, 89%) as a pale yellow oil. ^{1}H NMR (200 MHz, $CDCl_3$): $\delta = 7.38$ (d, $J = 8.0$ Hz, 2H), 7.10 (d, $J = 8.0$ Hz, 2H), 2.59 (t, $J = 7.5$ Hz, 2H), 1.58 (quint, $J = 7.5$ Hz, 2H), 1.46–1.12 (m, 18H), 0.89 (t, $J = 6.6$ Hz, 3H), 0.25 (s, 3H).

4-Ethynyldodecylbenzene (9): A solution of potassium fluoride (4.39 g, 75.6 mmol) in water (21 mL) was added to a solution of **8** (12.9 g 37.8 mmol) in dimethylformamide (300 mL). After stirring at room temperature for 3 h the reaction mixture was poured into water and extracted with toluene. The organic phase was washed with water, dried ($MgSO_4$), and concentrated under reduced pressure. The residue was purified by column chromatography on silica gel with petroleum ether to afford **9** (9.71 g, 95%) as a colorless oil. ^{1}H NMR (200 MHz, $CDCl_3$): $\delta = 7.42$ (d, $J = 8.1$ Hz, 2H), 7.14 (d, $J = 8.1$ Hz, 2H), 3.03 (s, 1H), 2.61 (t, $J = 7.7$ Hz, 2H), 1.61 (quint, $J = 7.7$ Hz, 2H), 1.44–1.11 (m, 18H), 0.90 (t, $J = 6.2$ Hz, 3H); ^{13}C NMR (50 MHz, $CDCl_3$): $\delta = 144.37$, 132.54, 128.87, 128.69, 119.87, 84.38, 76.88, 36.42, 32.46, 31.71, 30.19, 30.12, 30.02, 29.90, 29.78, 23.22, 14.60; FD-MS: *m*/*z* (%): 270.3 $[M]^+$ (100).

4-Bromo-4′-dodecyldiphenylacetylene (3c): Triphenylphosphine (948 mg, 3.62 mmol), copper iodide (691 mg, 3.63 mmol), and *trans*-dichlorobis(triphenylphosphine)palladium(II) (1.26 g, 1.80 mmol) in piperidine (280 mL) **9** (9.71 g, 35.9 mmol) was added dropwise to 4-bromoiodobenzene (11.2 g, 39.5 mmol). The resulting mixture was stirred at room temperature for 3 h under an argon atmosphere. The reaction mixture was poured into a

0947-6539/00/0623-4338 $ 17.50+.50/0 *Chem. Eur. J.* **2000**, *6*, No. 23

saturated ammonium chloride solution and extracted with dichloromethane. The organic phase was washed with concentrated ammonium chloride solution and water. After removing the solvent the residue was purified by column chromatography on silica gel with petroleum ether to yield **3c** (11.34 g, 74%) as colorless needles. M.p. 69.5 °C; ^{1}H NMR (500 MHz, $CDCl_3$): $\delta = 7.45$ (d, $J = 8.4$ Hz, 2H), 7.41 (d, $J = 8.1$ Hz, 2H), 7.356 (d, $J = 8.4$ Hz, 2H), 7.14 (d, $J = 8.1$ Hz, 2H), 2.59 (t, $J = 7.6$ Hz, 2H), 1.59 (t, $J = 7.6$ Hz, 2H), 1.33–1.20 (m, 18H), 0.87 (t, $J = 7.0$ Hz, 3H); ^{13}C NMR (125 MHz, $CDCl_3$): $\delta = 143.76$, 132.96, 131.57, 131.50, 128.51, 122.54, 122.22, 120.04, 90.79, 87.67, 35.92, 31.92, 31.20, 29.66, 29.63, 29.56, 29.47, 29.34, 29.24, 22.68, 14.10. anal. calcd (%) for $C_{26}H_{33}Br$: C 73.40, H 7.82, Br 18.78; found: C 73.85, H 7.71, Br 18.27.

1,3-Bis(4-dodecylphenyl)-propan-2-one (13b) as an example for the synthesis of substituted diphenylpropan-2-ones: A vigorously stirred mixture of 4-bromomethyldodecylbenzene (**12b**) (24 g, 71 mmol), iron pentacarbonyl (7.3 g, 37 mmol) benzyltriethylammoniumchloride (0.54 g, 1.93 mmol) and sodium hydroxide (12.3 g dissolved in 7 mL H_2O) in dichloromethane (170 mL) was heated at reflux overnight. After cooling to room temperature half concentrated HCl (130 mL) was added. The organic phase was then washed with 2 M HCl and water and dried ($MgSO_4$). The solvent was evaporated, and the residue was purified by column chromatography with petrol ether/CH_2Cl_2 3:1 to afford **13a**.

Compound **13a**: Yield: 53%; m.p. 116 °C; ^{1}H NMR (300 MHz, $CDCl_3$): $\delta = 7.47$ (d, $J = 8.4$ Hz, 4H), 7.04 (d, $J = 8.4$ Hz, 4H), 3.69 (s, 4H); ^{13}C NMR (75 MHz, $CDCl_3$): $\delta = 205.1$, 133.0, 132.3, 131.6, 121.7, 48.9; FD-MS: *m/z* (%): 367.7 $[M]^+$ (100); IR: $\tilde{\nu}$ = (KBr) 1715 (s), 1650 (m), 1488 (m), 1265 (m), 1012 (w), 738 (m), 704 (w); anal. calcd (%) for $C_{15}H_{12}Br_2O$: C 48.94, H 3.26; found: C 48.71, H 3.05.

Compound **13b**: Yield: 47%; m.p. 72–74 °C; ^{1}H NMR (300 MHz, $CDCl_3$): $\delta = 7.15$ (d, $J = 8.0$ Hz, 4H), 7.07 (d, $J = 8.0$ Hz, 4H), 3.69 (s, 4H), 2.60 (t, $J = 7.4$ Hz, 4H), 1.7–1.1 (m, 40H), 0.91 (d, $J = 7.4$ Hz, 6H); ^{13}C NMR (75 MHz, $CDCl_3$): $\delta = 206.5$, 142.2, 131.7, 129.8, 129.2, 49.2, 36.1, 42.4, 31.9, 30.0, 29.8, 23.2, 14.6; FD-MS: *m/z* (%): 546,4 $[M]^+$; IR (KBr): $\tilde{\nu} = 3421$ (s), 3043 (m), 2891 (s), 2849 (s), 1715 (s), 1467 (s); anal. calcd (%) for $C_{39}H_{62}O$: C 85.65, H 11.43; found: C 85.17, H 11.40.

4,4′-Didodecylbenzil (11): A mixture of 4,4′-didodecyldiphenylacetylene (50 g, 97 mmol) and iodine (12.2 g, 48 mmol) in dimethyl sulfoxide (250 mL) was stirred at 155 °C overnight. After cooling to room temperature, the reaction mixture was poured into an aqueous sodium thiosulfate solution (500 mL) and extracted with dichloromethane. The organic phase was washed with water and dried ($MgSO_4$). After evaporation of the solvent the residue was purified by column chromatography with petrol ether/dichloromethane 3:1 to yield **11** (55 g, 69%) as yellow crystals. M.p. 47 °C; ^{1}H NMR (300 MHz, $CDCl_3$): $\delta = 7.90$ (d, $J = 8.2$ Hz, 4H), 7.30 (d, $J = 8.2$ Hz, 4H), 2.68 (t, $J = 7.4$ Hz, 4H), 1.8–1.1 (m, 40H), 0.88 (d, $J = 7.6$ Hz, 6H); ^{13}C NMR (75 MHz, $CDCl_3$): $\delta = 194.8$, 151.2, 131.2, 128.8, 129.3, 36.5, 32.2, 31.3, 29.9, 29.8, 29.7, 29.6, 29.5, 23.0, 14.4; FD-MS: *m/z* (%): 546.3 $[M]^+$ (100); IR (KBr): $\tilde{\nu} = 3438$ (s), 2925 (m), 2850 (s), (s), 1671 (s), 1606 (s); anal. calcd (%) for $C_{39}H_{58}O_2$: C 83.46, H 10.69; found: C 83.49, H 10.89.

Tetrakis(4-dodecylphenyl)cyclopentadienone (14a) as an example for the synthesis of substituted tetraarylcyclopentadienones: A solution of potassium hydroxide (1.2 g, 22 mol) in ethanol (6 mL) was added to a refluxing solution of **11** (12 mg, 22 mmol) and 1,3-bis(4-dodecylphenyl)propan-2-one (10.81 g, 20 mmol) in ethanol (36 mL). After 5 min the reaction was cooled to 0 °C and the resulting purple oil was separated from the solvent. Column chromatography of this viscous oil with petrol ether/dichloromethane 4:1 afforded **14a** as a purple solid.

Compound **14a**: Yield: 43%; m.p. 55 °C; ^{1}H NMR (300 MHz, $CDCl_3$): $\delta = 7.19$ (d, $J = 8.2$ Hz, 4H), 7.05 (d, $J = 8.2$ Hz, 4H), 6.98 (d, $J = 8.2$ Hz, 4H), 6.83 (d, $J = 8.2$ Hz, 4H), 2.55 (t, $J = 7.5$ Hz, 4H), 1.8–1.1 (m, 40H), 0.91 (d, $J = 7.6$ Hz, 6H); ^{13}C NMR (75 MHz, $CDCl_3$): $\delta = 154.6$, 143.6, 142.5, 131.2, 130.4, 129.8, 128.9, 128.5, 128.3, 125.2, 36.2, 32.4, 31.7, 31.5, 30.2, 30.0, 29.9, 29.7, 23.2, 14.6; FD-MS: *m/z* (%): 1057.0 $[M]^+$ (100); IR (KBr): $\tilde{\nu} = 2924$ (s), 2853 (s), 1710 (s), 1465 (s); anal. calcd (%) for $C_{77}H_{116}O$: C 87.43, H 11.05; found: C 87.12, H 11.12.

Compound **14b**: Yield: 60%; m.p. 55 °C; ^{1}H NMR (300 MHz, $CDCl_3$): $\delta = 7.34$ (d, $J = 8.5$ Hz, 4H), 7.08 (d, $J = 8.5$ Hz, 4H), 6.97 (d, $J = 8.0$ Hz, 4H), 6.76 (d, $J = 8.0$ Hz, 4H), 2.54 (t, $J = 7.5$ Hz), 1.80–1.10 (m, 40H), 0.91 (t, $J = 6.8$ Hz, 6H); ^{13}C NMR (75 MHz, $CDCl_3$): $\delta = 199.6$, 155.3, 143.9, 131.6, 131.2, 130.2, 129.8, 129.2, 128.1, 123.9, 121.7, 35.8, 31.9, 31.0, 29.7, 29.5, 29.4, 29.2, 22.7, 14.1; FD-MS: *m/z* (%): 878.6 $[M]^+$ (100); IR (KBr): $\tilde{\nu} = 2924$ (s), 2853 (s), 1709 (s), 1486 (m), 1465 (m), 1072 (m), 1010 (m), 847 (w), 766 (w); anal. calcd (%) for $C_{53}H_{66}Br_2O$: C 72.44, H 7.52, Br 18.20; found: C 72.26, H 7.41, Br 17.80.

4-Bromo-4′,4″,4‴,4⁗,4⁗′-pentadodecylhexaphenylbenzene (4b) as an example for the synthesis of substituted hexaphenylbenzenes: A mixture of 4-bromo-4′-dodecyldiphenylacetylene (**11**) (4.00 g, 9.41 mmol) and tetra(4-dodecylphenyl)cyclopentadienone (**15b**) (10.0 g, 9.46 mmol) in diphenyl ether (15 mL) was heated at reflux for 16 h under an argon atmosphere. After cooling to room temperature ethanol (300 mL) was added to the reaction mixture. The solvent was decanted and the residual oil was purified by column chromatography on silica gel with petroleum ether/dichloromethane 10:1 to afford **4b**.

Compound **4b**: Yield: 71%; m.p. 35.5 °C; ^{1}H NMR (500 MHz, $CDCl_3$): $\delta =$ 6.93 (d, $J = 8.2$ Hz, 2H), 6.66–6.61 (m, 16H), 6.59 (d, $J = 7.9$ Hz, 6H), 2.35 (t, $J = 7.6$ Hz, 4H), 2.32 (t, $J = 7.6$ Hz, 6H), 1.43–1.06 (m, 100H), 0.87 (t, $J = 6.9$ Hz, 15H); ^{13}C NMR (125 MHz, $CDCl_3$): $\delta = 140.85$, 140.57, 140.25, 140.11, 139.48, 139.19, 138.80, 138.06, 137.99, 137.84, 133.24, 131.30, 129.56, 126.77, 126.50, 119.06, 35.35, 35.32, 31.94, 31.23, 31.14, 29.76, 29.75, 29.69, 29.54, 29.38, 28.88, 28.82, 22.69, 14.09; FD-MS: *m/z* (%): 1454.5 $[M]^+$ (100); anal. calcd (%) for $C_{102}H_{149}Br$: C 84.19, H 10.32, Br 5.49; found: C 84.30, H 10.43, Br 5.40.

Compound **4c**: Oil; yield: 76%; ^{1}H NMR (250 MHz, $CDCl_3$): $\delta = 6.97$ (d, $J = 8.5$ Hz, 4H), 6.65 (d, $J = 8.5$ Hz, 4H), 6.62–6.60 (m, 16H), 2.38–2.28 (m, 8H), 1.38–1.04 (m, 80H), 0.88–0.83 (m, 12H); ^{13}C NMR (63 MHz, $CDCl_3$): $\delta = 140.7$, 140.0, 139.3, 139.2, 138.9, 138.1, 137.3, 137.1, 132.7, 130.8, 129.5, 126.4, 126.2, 119.1, 34.9, 31.6, 30.8, 30.7, 29.4, 29.3, 29.2, 29.0, 28.5, 28.4, 22.3, 13.7; FD-MS: *m/z* (%): 1365.1 $[M]^+$ (100).

Compound **4d**: Yield: 74%; m.p. 71 °C; ^{1}H NMR (300 MHz, $CDCl_3$): $\delta =$ 6.88 (d, $J = 8.5$ Hz, 4H), 6.61 (d, $J = 8.5$ Hz, 4H), 6.58–6.56 (m, 16H), 2.29 (t, $J = 7.3$ Hz, 8H), 1.35–1.04 (m, 80H), 0.91 (t, $J = 6.8$ Hz, 12H); ^{13}C NMR (75 MHz, $CDCl_3$): $\delta = 141.6$, 140.8, 140.4, 138.9, 134.6, 132.5, 130.8, 128.1, 120.2, 36.7, 33.3, 32.5, 31.1, 31.0, 30.9, 30.7, 30.1, 24.1, 15.6; FD-MS: *m/z* (%): 1365.1 $[M]^+$ (100); anal. calcd (%) for $C_{90}H_{124}Br_2$: C 79.19, H 9.09, Br 11.72; found: C 79.24, H 8.95, Br 11.57.

2-Bromo-5,8,11,14,17-pentadodecylhexa-*peri*-hexabenzocoronene (2a) as an example for the synthesis of substituted hexa-*peri*-hexabenzocoronenes: A solution of iron(III)chloride (3.87 g, 23.9 mmol) in nitromethane (30 mL) was added dropwise to a stirred solution of 4-bromo-4′,4″,4‴,4⁗,4⁗′-pentadodecylhexaphenylbenzene (**4b**) (2.03 g, 140 mmol) in dichloromethane (400 mL). An argon stream was bubbled through the reaction mixture throughout the entire reaction. After stirring another 30 min the reaction was quenched with methanol (200 mL). The precipitate was filtered, washed with methanol (200 mL), and dried under reduced pressure. The crude product was purified by column chromatography on silica gel with hot toluene/petroleum ether to afford **2a**.

Compound **2a**: Yield: 93%; ^{1}H NMR (500 MHz, 50% $CDCl_3/CS_2$): $\delta =$ 7.99 (s, 2H), 7.86 (s, 2H), 7.75 (s, 2H), 7.61 (s, 2H), 7.53 (s, 2H), 7.40 (s, 2H), 2.94 (m, 2H), 2.73 (m, 4H), 2.51 (m, 4H), 2.03 (m, 2H), 1.86 (m, 4H), 1.78–1.24 (m, 94H), 0.95–0.87 (m, 15H); ^{13}C NMR (125 MHz, 50% $CDCl_3/CS_2$): $\delta = 138.86$, 138.71, 138.64, 130.10, 128.82, 128.58, 128.29, 128.17, 127.03, 122.24, 121.99, 121.86, 121.76, 121.70, 120.64, 120.38, 120.22, 120.14, 120.00, 119.91, 118.40, 118.06, 117.81, 117.10, 37.40, 37.20, 36.86, 32.67, 32.50, 32.21, 32.08, 31.96, 30.43, 30.34, 30.27, 30.18, 30.11, 30.08, 30.02, 29.99, 29.91, 29.56, 22.86, 14.19; FD-MS: *m/z* (%): 1442.1 $[M]^+$ (100); anal. calcd (%) for $C_{102}H_{149}Br$: C 84.19, H 10.32, Br 5.49; found: C 84.26, H 10.39, Br 5.17.

Compound **2b**: Yield: 89%; ^{1}H NMR (250 MHz, 50% $CDCl_3/CS_2$): $\delta =$ 7.77 (s, 2H), 7.53 (s, 2H), 7.32 (s, 2H), 7.03 (s, 2H), 6.91 (s, 2H), 6.85 (s, 2H), 2.86 (t, $J = 7.2$ Hz, 4H), 2.52 (t, $J = 7.2$ Hz, 4H), 2.09–1.90 (m, 4H), 1.85–1.32 (m, 76H), 1.02–0.97 (m, 12H); ^{13}C NMR (125 MHz, $CDCl_3$): $\delta =$ 139.08, 138.58, 129.78, 129.13, 128.48, 128.29, 127.86, 126.44, 122.60, 122.22, 121.10, 120.92, 120.87, 120.69, 120.40, 120.00, 119.87, 117.54, 117.01, 116.00, 110.39, 37.67, 37.28, 32.93, 32.61, 32.42, 30.85, 30.79, 30.64, 30.59, 30.56, 30.54, 30.45, 30.11, 23.49, 14.71; FD-MS: *m/z* (%): 1353.4 $[M]^+$ (100); anal. calcd (%) for $C_{90}H_{112}Br_2$: C 79.86; H 8.34, Br 11.81; found: C 79.88, H 8.46, Br: 11.40.

Compound **2c**: Yield: 87%; ^{1}H NMR (300 MHz, 50% $CDCl_3/CS_2$): $\delta = 7.51$ (s, 4H), 7.11 (s, 8H), 2.42 (t, $J = 7.4$ Hz, 8H), 1.71–1.40 (m, 80H), 0.98 (t, $J = 6.8$ Hz, 12H); ^{13}C NMR (75 MHz, $CDCl_3$): $\delta = 138.8$, 130.0, 127.8, 126.8, 122.6, 121.4, 121.1, 120.8, 120.2, 117.2, 116.9, 37.3, 32.8, 32.6, 30.9, 30.8, 30.7,

30.6, 30.3, 23.7, 15.0; FD-MS: *m/z* (%): 1353.4 $[M]^+$ (100); anal. calcd (%) for $C_{90}H_{112}Br_2$: C 79.86, H 8.34, Br 11.81; found: C 79.77, H 8.22, Br 11.32.

2-(*N*-Undecyl)amino-5,8,11,14,17-pentadodecylhexa-*peri*-hexabenzocoronene (15a) as an example for the synthesis of amino-substituted hexa-*peri*-hexabenzocoronenes: A mixture of 2-bromo-5,8,11,14,17-pentadodecylhexa-*peri*-hexabenzocoronene (**2a**) (104 mg, 0.0718 mmol), undecylamine (0.45 mL, 358 mg, 2.09 mmol), sodium *tert*-butoxide (242 mg, 2.52 mmol), tris(dibenzylideneacetone)-dipalladium(0) (7.1 mg, 0.0078 mmol), and (*R*)-BINAP ((*R*)-(+)-2,2′-bis(diphenylphosphino)-1,1′-binaphthyl) (13 mg, 0.021 mmol) in toluene (10 mL) was heated at 80 °C for 4 h under an argon atmosphere. The resulting mixture was purified by column chromatography on silica gel with hot toluene/petroleum ether to afford the 4-undecylaminohexabenzocoronene (83 mg, 75%) as yellow crystals.

Compound **15a**: ^{1}H NMR (500 MHz, 50% $CDCl_3/CS_2$): $\delta = 8.30$ (s, 4H), 8.26 (s, 2H), 8.20 (s, 2H), 7.97 (s, 2H), 7.38 (s, 2H), 3.23 (t, $J = 6.6$ Hz, 2H), 2.97 (t, $J = 8.7$ Hz, 4H), 2.95 (t, $J = 8.7$ Hz, 2H), 2.85 (t, $J = 7.8$ Hz, 4H), 2.00–1.78 (m, 12H), 1.68–1.22 (m, 106H), 0.95–0.85 (m, 18H); ^{13}C NMR (125 MHz, 50% $CDCl_3/CS_2$): $\delta = 145.79$, 139.31, 139.13, 139.03, 130.52, 129.56, 129.50, 129.31, 129.04, 123.25, 123.15, 123.11, 120.80, 120.68, 119.69, 119.31, 118.31, 118.09, 117.68, 105.49, 44.19, 37.35, 37.20, 32.56, 32.42, 32.07, 32.03, 30.30, 30.24, 30.18, 30.05, 30.00, 29.92, 29.89, 29.84, 29.55, 29.51, 27.77, 22.85, 22.81, 14.15; FD-MS: *m/z* (%): 1533.1 $[M]^+$ (100); anal. calcd (%) for $C_{113}H_{161}N$: C 88.50, H 10.58, N 0.91; found: C 88.25, H 10.16, N 0.87.

Compound **15b**: ^{1}H NMR (500 MHz, 50% $CDCl_3/CS_2$): $\delta = 8.58$ (s, 2H), 8.55 (s, 2H), 8.51 (s, 2H), 8.28 (s, 2H), 7.67 (s, 2H),7.36 (s, 2H), 3.72 (m, 2H), 3.28 (t, $J =$ 7.2 Hz, 4H), 3.09 (t, $J = 8.0$ Hz, 4H), 3.02 (t, $J =$ 8.1 Hz, 4H), 2.02–1.92 (m, 12H), 1.86–1.20 (m, 102H), 0.90–0.85 (m, 18H); ^{13}C NMR (125 MHz, 50% $CDCl_3/CS_2$): $\delta = 145.60$, 139.09, 139.01, 130.54, 130.26, 129.54, 129.51, 129.47, 129.33, 123.51, 123.40, 120.86, 120.79, 120.73, 118.78, 118.54, 118.34, 117.91, 105.67, 105.44, 44.12, 37.37, 37.27, 32.58, 32.47, 32.05, 30.22, 30.05, 30.02, 29.95, 29.86, 29.54, 27.73, 22.90, 14.21; FD-MS: *m/z* (%): 1534.2 $[M]^+$ (100); anal. calcd (%) for $C_{112}H_{160}N_2$: C 87.66, H 10.51, N 1.83; found: C 87.64, H 10.53, N 1.81.

Compound **15c**: ^{1}H NMR (500 MHz, 50% $CDCl_3/CS_2$): $\delta = 8.46$ (s, 4H), 8.30 (s, 4H), 7.73 (s, 4H), 3.85 (br m, 2H), 3.37 (t, $J =$ 6.6 Hz, 4H), 3.01 (t, $J = 7.7$ Hz, 8H), 1.98–1.85 (m, 12H), 1.59–1.32 (m, 104H), 0.90–0.85 (m, 18H); ^{13}C NMR (125 MHz, 50% $CDCl_3/CS_2$): $\delta = 145.2$, 138.5, 130.0, 129.0, 128.7, 122.8, 120.2, 118.4, 117.8, 117.4, 105.0, 43.4, 36.4, 31.5, 31.2, 31.1, 29.3, 29.2, 29.1, 29.0, 28.9, 28.6, 26.8, 22.0, 13.3; FD-MS: *m/z* (%): 1534.2 $[M]^+$ (100); anal. calcd (%) for $C_{112}H_{160}N_2$: C 87.66, H 10.51; found: C 87.72, H 10.41.

2-Piperidino-5,8,11,14,17-pentadodecylhexa-*peri*-hexabenzocoronene (17): A mixture of 2-bromo-5,8,11,14,17-pentadodecylhexa-*peri*-hexabenzocoronene (**2a**) (107 mg, 0.074 mmol), piperidine (0.21 mL, 181 mg, 2.12 mmol), sodium *tert*-butoxide (242 mg, 2.52 mmol), tris(dibenzylideneacetone)dipalladium(0) (7.9 mg, 0.0086 mmol), and (*R*)-BINAP ((*R*)-(+)-2,2′-bis(diphenylphosphino)-1,1′-binaphthyl) (16 mg, 0.026 mmol) in toluene (10 mL) was heated at 80 °C for 4 h under an argon atmosphere. The resulting mixture was purified by column chromatography on silica gel with hot toluene/petroleum ether to afford **17** (83 mg, 78%) as yellow crystals. ^{1}H NMR (500 MHz, 50% $CDCl_3/CS_2$): $\delta = 8.25$ (s, 2H), 8.22 (s, 2H), 8.16 (s, 2H), 8.15 (s, 2H), 8.11 (s, 2H), 8.10 (s, 2H), 3.57 (t, $J = 5.3$ Hz, 4H), 2.95 (t, $J = 8.1$ Hz, 4H), 2.875 (t, $J = 7.5$ Hz, 4H), 2.86 (t, $J = 7.5$ Hz, 2H), 2.10–2.04 (m, 4H), 1.98–1.83 (m, 12H), 1.66–1.23 (m, 90H), 0.92–0.85 (m, 15H); ^{13}C NMR (125 MHz, 50% $CDCl_3/CS_2$): $\delta = 149.80$, 139.26, 139.05, 130.45, 129.47, 129.33, 129.11, 123.21, 122.88, 120.89, 120.76, 120.64, 119.34, 119.22, 119.19, 118.54, 118.46, 109.95, 51.64, 37.35, 37.28, 32.62, 32.46, 32.04, 30.22, 30.05, 30.00, 29.92, 29.84, 29.51, 26.63, 24.79, 22.82, 14.16; FD-MS: *m/z* (%): 1446.6 $[M]^+$ (100); anal. calcd (%) for $C_{107}H_{147}N$: C 88.80, H 10.24, N 0.97; found: C 88.21, H 10.26, N 0.91.

2-Cyclohexyloxyhexabenzocoronene (16): After stirring a mixture of cyclohexanol (1.14 g, 11.4 mmol) and sodium hydride (338 mg, 14.1 mmol), in toluene (50 mL) at room temperature for 1 h, 2-bromo-5,8,11,14,17-pentadodecylhexa-*peri*-hexabenzocoronene (**2a**) (503 mg, 0.348 mmol), tris(dibenzylideneacetone)dipalladium(0) (33 mg, 0.036 mmol), and (*R*)-BINAP ((*R*)-(+)-2,2′-bis(diphenylphosphino)-1,1′-binaphthyl) (67 mg, 0.11 mmol) was added to the mixture. The resulting mixture was stirred at 80 °C for 2 h under an argon atmosphere. The reaction mixture was poured into water and extracted with hot toluene. The organic phase was washed with water, dried ($MgSO_4$), and concentrated under reduced pressure. The residue was purified by column chromatography on silica gel with petroleum ether/carbon disulfide 3:1 and hot toluene/petroleum ether 1:1 to afford **16** (87 mg, 17%) as yellow crystals. ^{1}H NMR (500 MHz, 50% $CDCl_3/CS_2$): $\delta = 8.27$ (s, 2H), 8.26 (s, 2H), 8.19 (s, 2H), 8.17 (s, 4H), 8.14 (s, 2H), 4.76 (m, 1H), 2.98 (t, $J = 8.4$ Hz, 4H), 2.93 (t, $J = 8.4$ Hz, 2H), 2.91 (t, $J = 8.4$ Hz, 4H), 2.39–2.32 (m, 2H), 2.16–2.08 (m, 2H), 2.00–1.88 (m, 14H), 1.85–1.77 (m, 2H), 1.76–1.24 (m, 90H), 0.892 (t, $J = 6.6$ Hz, 15H); ^{13}C NMR (125 MHz, 50% $CDCl_3/S_2$): $\delta = 155.57$, 139.31, 139.14, 131.22, 129.42, 129.31, 129.20, 129.13, 129.10, 123.08, 122.79, 121.13, 120.89, 120.72, 120.67, 119.78, 119.19, 118.67, 118.48, 109.00, 75.35, 37.26, 37.23, 32.46, 32.43, 32.38, 32.32, 32.04, 30.19, 30.16, 30.04, 30.00, 29.93, 29.85, 29.53, 26.17, 24.06, 22.89, 14.20; FD-MS: *m/z* (%): 1462.0 $[M]^+$ (100); anal. calcd (%) for $C_{108}H_{148}O$: C 88.70, H 10.20; found: C 88.27, H 10.22.

2-Methoxycarbonyl-5,8,11,14,17-pentadodecylhexa-*peri*-hexabenzocoronene (18a) as an example for the synthesis of methylester-substituted hexa-*peri*-hexabenzocoronenes: A mixture of 2-bromo-5,8,11,14,17-pentadodecylhexa-*peri*-hexabenzocoronene (**10**) (530 mg, 0.367 mmol), triphenylphosphine (100 mg, 0.383 mmol), triethylamine (1.06 g, 10.1 mmol), methanol (703 mg, 21.9 mmol), and *trans*-dichlorobis(triphenylphosphine)palladium(II) (131 mg, 0.186 mmol) in tetrahydrofuran (20 mL) was stirred at 100 °C for 5 d under a carbon monoxide atmosphere (5 atm) in a 40 mL autoclave. After cooling the reaction mixture the solvent was removed under reduced pressure. The residue was purified by column chromatography on silica gel with hot toluene/petroleum ether to afford 2-methoxycarbonyl-5,8,11,14,17-pentadodecylhexa-*peri*-hexabenzocoronene (325 mg, 62%) as orange yellow crystals.

Compound **18a**: ^{1}H NMR (500 MHz, 50% $CDCl_3/CS_2$): $\delta = 8.47$ (s, 2H), 7.80 (s, 2H), 7.74 (s, 2H), 7.71 (s, 2H), 7.66 (s, 2H), 7.63 (s, 2H), 4.14 (s, 3H), 2.76 (t, $J = 8.1$ Hz, 2H), 2.66 (t, $J = 8.1$ Hz, 4H), 2.59 (t, $J = 8.1$ Hz, 4H), 1.88 (q, $J = 8.1$ Hz, 2H), 1.83–1.72 (m, 8H), 1.64–1.23 (m, 90H), 0.93–0.88 (m, 15H); ^{13}C NMR (125 MHz, 50% $CDCl_3/CS_2$): $\delta = 167.15$, 139.16, 138.90, 128.93, 128.62, 128.52, 128.46, 128.26, 126.43, 125.15, 121.89, 120.65, 120.49, 120.41, 120.25, 119.28, 119.04, 118.22, 117.31, 51.86, 37.24, 37.12, 37.03, 32.49, 32.41, 32.37, 32.07, 31.96, 30.39, 30.34, 30.12, 30.08, 30.05, 29.98, 29.89, 29.55, 22.86, 14.18; FD-MS: *m/z* (%): 1422.3 $[M]^+$ (100); anal. calcd (%) for $C_{104}H_{140}O_2$: C 87.83, H 9.92; found: C 87.63, H 9.03.

Compound **18b**: ^{1}H NMR (250 MHz, CD_2Cl_2/CS_2): $\delta = 7.83$ (s, 2H), 7.78 (s, 2H), 7.61 (s, 2H), 7.50 (s, 2H), 7.36 (s, 2H), 7.25 (s, 2H), 3.99 (s, 3H), 2.71 (t, $J = 7.5$ Hz, 4H), 2.49 (t, $J = 7.2$ Hz, 4H), 1.91–1.25 (m, 80H), 1.03–0.88 (m, 12H); ^{13}C NMR (125 MHz, CD_2Cl_2/CS_2): $\delta = 167.23$, 140.36, 140.21, 129.76, 129.64, 129.21, 128.79, 128.50, 126.41, 122.41, 122.21, 121.92, 121.61, 121.45, 119.66, 119.40, 118.43, 52.81, 38.56, 38.29, 33.61, 33.37, 31.94, 31.90, 31.66, 31.56, 31.52, 31.43, 31.10, 24.50, 15.72; FD-MS: *m/z* (%): 1311.9 $[M]^+$ (100); anal. calcd (%) for $C_{94}H_{118}O_4$: C 86.06, H 9.07; found: C 86.03, H 8.98.

2-Cyano-5,8,11,14,17-pentadodecylhexa-*peri*-hexabenzocoronene (19a): A mixture of 2-bromo-5,8,11,14,17-pentadodecylhexa-*peri*-hexabenzocoronene (315 mg, 0.219 mmol) and copper cyanide (4.10 g, 45.7 mmol) in *N*-methyl-2-pyrrolidinone (30 mL) was heated at 185 °C for 20 h under an argon atmosphere. The reaction mixture was poured into 10% ammonium hydroxide solution. The precipitated crystals were collected by filtration, washed with water and purified by column chromatography on silica gel with CS_2/petroleum ether 1:1 and toluene/petroleum ether 1:1 to afford the 2-cyano-5,8,11,14,17-pentadodecylhexa-*peri*-hexabenzocoronene (184 mg, 61%) as yellow crystals. ^{1}H NMR (500 MHz, 50% $CDCl_3/CS_2$): $\delta = 7.92$ (s, 2H), 7.76 (s, 2H), 7.35 (s, 2H), 7.16 (s, 2H), 7.08 (s, 2H), 6.82 (s, 2H), 2.89 (t, $J = 8.2$ Hz, 2H), 2.66 (t, $J = 8.2$ Hz, 4H), 2.17 (t, $J = 8.2$ Hz, 4H), 1.97 (quint, $J = 8.2$ Hz, 2H), 1.80 (quint, $J = 8.2$ Hz, 4H), 1.71–1.25 (m, 94H), 0.98–0.87 (m, 15H); ^{13}C NMR (125 MHz, 50% $CDCl_3/CS_2$): $\delta = 139.44$, 138.82, 138.57, 128.75, 128.14, 127.76, 127.60, 127.53, 125.92, 124.25, 121.37, 121.30, 121.12, 120.68, 120.35, 120.29, 120.15, 119.98, 119.22, 118.67, 117.80, 117.36, 115.43, 107.19, 37.27, 37.09, 36.41, 32.68, 32.45, 32.08, 31.98, 31.81, 30.43, 30.36, 30.24, 30.20, 30.16, 30.11, 30.07, 30.04, 30.01, 29.92, 29.58, 22.91, 14.21; FD-MS: *m/z* (%): 1388.4 $[M]^+$ (100); anal. calcd (%) for $C_{103}H_{137}N$: C 89.05, H 9.94, N 1.01; found: C 88.41, H 10.03, N 0.90.

Acknowledgements

Financial support by the European Commission (TMR-Program Sisitomas) and by the Volkswagen Stiftung is gratefully acknowledged.

  0947-6539/00/0623-4340 $ 17.50+.50/0

[1] a) C. Destrade, H. T. Nguyen, H. Gasparoux, J. Malthete, A. M. Levelut, *Mol. Cryst. Liq. Cryst.* **1981**, *71*, 111.

[2] a) C. Carfanga, A. Roviello, A. Sirigu, *Mol. Cryst. Liq. Cryst.* **1985**, *122*, 151; b) K. S. Raja, S. Ramakrishnan, V. A. Raghunathan, *Chem. Mater.* **1997**, *9*, 1630.

[3] S. Zamir, D. Singer, N. Spielberg, E. J. Wachtel, H. Zimmermann, R. Poupko, Z. Luz, *Liq. Cryst.* **1996**, *21*, 39.

[4] S. Chandrasekhar, B. K. Sadashiva, K. A. Suresh, *Pramana* **1977**, *9*, 471.

[5] N. Boden, R. J. Bushby, J. Clements, M. V. Jesudason, P. F. Knowles, G. Williams, *Chem. Phys. Lett.* **1988**, *152*, 94.

[6] D. Adam, F. Closs, T. Frey, D. Funhoff, D. Haarer, H. Ringsdorf, P. Schuhmacher, K. Siemensmeyer, *Phys. Rev. Lett.* **1993**, *70*, 457.

[7] a) N. Boden, R. J. Bushby, A. N. Cammidge, J. Clements, R. Luo, K. J. Donovan, *Mol. Cryst. Liq. Cryst.* **1995**, *261*, 251; b) D. Haarer, D. Adam, J. Simmerer, F. Closs, D. Funhoff, L. Häussling, K. Siemensmeyer, H. Ringsdorf, P. Schuhmacher, *Mol. Cryst. Liq. Cryst.* **1994**, *252*, 155; c) D. Adam, P. Schuhmacher, J. Simmerer, L. Häussling, K. Siemensmeyer, K. H. Etzbach, H. Ringsdorf, D. Haarer, *Nature* **1994**, *371*, 141; d) A. M. Van de Craats, M. P. de Haas, J. M. Warman, *Synth. Met.* **1997**, *86*, 2125.

[8] P. Herwig, C. W. Kayser, K. Müllen, H. W. Spiess, *Adv. Mater.* **1996**, *8*, 510.

[9] A. M. Van de Craats, J. M. Warman, K. Müllen, Y. Geerts, J. D. Brand, *Adv. Mater.* **1998**, *10*, 36.

[10] D. M. Cyr, B. Venkatamaran, G. W. Flynn, *Chem. Mater.* **1996**, *8*, 1600.

[11] J. P. Rabe, S. Buchholz, L. Askadskaya, *Synth. Met.* **1993**, *54*, 339.

[12] D. M. Walba, F. Stefens, D. C. Parks, N. A. Clark, M. D. Wand, *Science* **1995**, *267*, 1144.

[13] A. Stabel, P. Herwig, K. Müllen, J. P. Rabe, *Angew. Chem.* **1995**, *107*, 1768; *Angew. Chem. Int. Ed. Engl.* **1995**, *34*, 1609.

[14] L. Askadskaya, C. Boeffel, J. P. Rabe, *Ber. Bunsenges. Phys. Chem.* **1993**, *97*, 517.

[15] BF_3/Et_2O, $SbCl_5/CH_2Cl_2$, $MoCl_5$, $FeCl_3$/nitromethane.

[16] V. S. Iyer, M. Wehmeier, J. D. Brand, M. A. Keegstra, K. Müllen, *Angew. Chem.* **1997**, *109*, 1675; *Angew. Chem. Int. Ed. Engl.* **1997**, *36*, 1603.

[17] K. P. C. Vollhardt, *Acc. Chem. Res.* **1977**, *10*, 1.

[18] a) W. Dilthey, W. Schommer, H. Dierichs, O. Trösken, *Ber. Dtsch. Chem. Ges.* **1933**, *66*, 1627; b) W. Dilthey, G. Hurtig, *Ber. Dtsch. Chem. Ges.* **1934**, *67*, 2004.

[19] H. J. Barber, R. Slack, *J. Chem. Soc.* **1944**, 612.

[20] M. Kumada, K. Sumitani, K. Tamao, *J. Am. Chem. Soc.* **1972**, *94*, 4374.

[21] S. Bance, H. J. Barber, A. M. Woolman, *J. Chem. Soc.* **1943**, 1.

[22] S. Taskahashi, Y. Kuroyama, K. Sonogashira, N. Hagihara, *Synthesis* **1980**, 627.

[23] 4-Bromo-dodecylbenzene was easily available by a Friedel–Crafts acylation of lauroyl chloride and bromobenzene, followed by a Wolff–Kishner reduction of the resulting ketone.

[24] G. Pattenden, G. M. Robertson, *Tetrahedron Lett.* **1986**, *27*, 399.

[25] M. S. Yusubov, V. D. Filimonov, *Synthesis* **1991**, 131.

[26] a) Y. Kimura, Y. Tomito, S. Nakanishi, Y. Otsuji, *Chem. Lett.* **1979**, 321; b) H. des Abbayes, J. Clement, J. Laurent, G. Tanguy, N. Thilmont, *Organometallics* **1988**, *7*, 2293.

[27] a) M. A. Ogliaruso, M. G. Romanelli, E. I. Becker, *Chem. Rev.* **1965**, *65*, 261; b) W. Broser, J. Reusch, H. Kurreck, P. Siegle, *Chem. Ber.* **1969**, *102*, 1715.

[28] a) P. Kovacic, A. Kyriakis, *J. Am. Chem. Soc.* **1963**, *85*, 454; b) P. Kovacic, R. M. Lange, *J. Org. Chem.* **1963**, *28*, 968.

[29] P. Kovacic, F. W. Koch, *J. Org. Chem.* **1963**, *28*, 1864.

[30] J. P. Wolfe, S. Wagaw, S. L. Buchwald, *J. Am. Chem. Soc.* **1996**, *118*, 7215.

[31] According to mass spectrometry of the crude reaction product, conversion is quantitative. Some material is lost on the chromatography column, due to irreversible adsorption on the silica gel.

[32] M. Palucki, P. Wolfe, S. L. Buchwald, *J. Am. Chem. Soc.* **1997**, *119*, 3395.

[33] A. Schoenberg, I. Bartoletti, R. F. Heck, *J. Org. Chem.* **1974**, *39*, 3318.

[34] G. P. Ellis, T. M. Romney-Alexander, *Chem. Rev.* **1987**, *87*, 779.

[35] A detailed discussion of the UV/Vis spectra of the new HBC-derivates will be subject of a future publication.

[36] The first DSC cycle is not reversible in some cases. This is, presumably, due to solvent effect that induce a crystal structure, which can not be observed by thermal treatment.

[37] a) Y. Bouligand, *J. Phys.* **1980**, *41*, 1307; b) S. Chandrasekhar, G. S. Ranganath, *Adv. Phys.* **1986**, *35*, 507.

[38] a) A. R. A. Palmans, J. A. J. M. Vekemans, H. Fischer, R. A. Hikmet, E. W. Meijer, *Chem. Eur. J.* **1997**, *3*, 300; b) O. Fernández, G. de la Torre, F. Fernández-Lázaro, J. Barberá, T. Torres, *Chem. Mater.* **1997**, *9*, 3017.

[39] a) A. M. Levelut, F. Hardouin, H. Gasproux, C. Destrade, N. H. Tinh, *J. Phys.* **1981**, *42*, 147; b) A. M. Levelut, *J. Chim. Phys.* **1983**, *80*, 149.

[40] Alignment of the samples in the mesophase by mechanical shearing leads to texture effects during the X-ray measurements, which influences the intensity of the 001-reflection.

[41] J. P. Rabe, S. Buchholz, *Science* **1991**, *253*, 424.

[42] J. P. Rabe, S. Buchholz, L. Askadskaya, *Physica Scripta* **1993**, *T49*, 260.

[43] J. P. Rabe, S. Buchholz, *Phys. Rev. Lett.* **1991**, *66*, 2096.

[44] A. Stabel, R. Heinz, F. C. De Schryver, J. P. Rabe, *J. Phys. Chem.* **1995**, *99*, 505.

[45] By varying the tunneling current it is possible to observe the two-dimensional lattice of molecules on the one hand (U_{bias}: 1.0–1.8 V) and the substrate lattice on the other hand (U_{bias}: 30–200 mV). This method has been described in [11], [41] and [49].

[46] See also, R. Epsch, PhD thesis, Humboldt University Berlin, **1999**.

[47] D. P. E. Smith, J. K. H. Hörber, G. Binning, H. Nejoh, *Nature* **1990**, *344*, 641.

[48] J. Foster, J. Frommer, *Nature* **1988**, *333*, 542.

[49] A. Stabel, R. Heinz, J. P. Rabe, G. Wegner, F. C. de Schryver, D. Corens, W. Dehaen, C. Süling, *J. Phys. Chem.* **1995**, *99*, 8890.

[50] Crystallographic data of unsubstituted HBCs and also of longer alkyl chains have been used to determine the theoretical value of the area, which one flat lying molecule needs. The van der Waals contour of these molecules has been determined from a) A. Stabel, R. Heinz, J. P. Rabe, G. Wegner, F. C. De Schryver, D. Corens, W. Dehaen, C. Süling, *J. Phys. Chem.* **1995**, *99*, 8690; b) G. C. McGonigal, R. H. Bernhardt, D. J. Thomson, *Appl. Phys. Lett.* **1990**, *57*, 28; c) U. Zimmermann, N. Karl, *Surf. Sci.* **1992**, *268*, 296.

[51] D. M. Cyr, B. Venkataraman, G. W. Flynn, A. Black, G. M. Whitesides, *J. Phys. Chem.* **1996**, *100*, 13747.

[52] L. Ciancarlo, D. Cyr, K. Muyskens, G. W. Flynn, *Langmuir* **1998**, *14*, 1465.

[53] C. Claypool, F. Faglioni, W. A. Goddard III, H. B. Gray, N. S. Lewis, R. A. Marcus, *J. Phys. Chem. B* **1997**, *101*, 5978.

[54] A. Belaaraj, Y. Haget, Nguyen-Ba-Chanh, *J. Appl. Crystallogr.* **1984**, *17*, 211; H. J. Milledge, L. M. Pant, *Acta Crystallogr.* **1960**, *13*, 285.

[55] Intermolecular forces between fluorine atoms are unfavorable because of the extreme high electronegativity of fluorine. Therefore, instead of attractive interactions between neighboring flourine end groups F···H contacts frequently occur.

[56] P. Seurin, D. Guillon, A. Skoulios, *Mol. Cryst. Liq. Cryst.* **1981**, *71*, 51.

[57] A. Zinsou, H. Strzelecka, C. Jallabert, A. M. Levelut, *Liq. Cryst.* **1994**, *17*, 513.

[58] a) N. Boden, R. C. Borner, R. J. Bushby, A. N. Cammige, *Liq. Cryst.* **1993**, *15*, 851; b) N. Boden, R. J. Bushby, A. N. Cammige, *J. Am. Chem. Soc.* **1995**, *117*, 924; c) N. Boden, R. C. Borner, R. J. Bushby, Z. B. Lu, *Liq. Cryst.* **1998**, *25*, 851.

[59] J. Krim, J. Suzanne, H. Shechter, R. Wang, H. Taub, *Surf. Sci.* **1985**, *162*, 446.

[60] A. I. Kitaigorodski, *Molecular crystals and molecules*, Academic Press, New York **1973**.

[61] The measuring time is limited due to the onset of three-dimensional growth with time, which caused an increased friction by the additional layers. This perturbation can be reduced by decreasing of the concentration, but in this case the time which is necessary for the formation of the first monolayer is extremely high. In the present case, measuring times in the range of 1–2 h are typical.

[62] S. L. Price, A. J. Stone, J. Lucas, R. S. Rowland, A. E. Thornley, *J. Am. Chem. Soc.* **1994**, *116*, 4910.

[63] S. C. Nyburg, W. Wong-Hg, *Proc. R. Soc. London* **1979**, *A367*, 29; S. C. Nyburg, C. H. Faerman, *Acta Crystallogr.* **1985**, *B41*, 274.

[64] G. R. Desiraju, R. Parthasarathy, *J. Am. Chem. Soc.* **1989**, *111*, 8725.
[65] N. Ramasubbu, R. Parthasarathy, P. Murray-Rust, *J. Am. Chem. Soc.* **1986**, *108*, 4308.
[66] A. T. Christensen, K. O. Strømme, *Acta Crystallogr.* **1969**, *B25*, 657.
[67] G. R. Desiraju, Crystal Engineering: *The Design of Organic Solids*, Elsevier, Amsterdam, **1989**.
[68] K. Besocke, *Surf. Sci.* **1989** *181*, 145.
[69] J. Frohn, J. F. Wolf, K. Besocke, M. Teske, *Rev. Sci. Instrum.* **1989**, *60*, 1200.
[70] W. Mizutani, M. Shigeno, M. Ono, K. Kajimura, *Appl. Phys. Lett.* **1990**, *56*, 1974.

Received: July 13, 1999
Revised version: March 14, 2000 [F1910]

  0947-6539/00/0623-4342 $ 17.50+.50/0